Properties and Applications of the β Phase Poly(vinylidene fluoride)

Liuxia Ruan [1], Xiannian Yao [1], Yufang Chang [2], Lianqun Zhou [3], Gaowu Qin [1] and Xianmin Zhang [1,*]

[1] Key Laboratory for Anisotropy and Texture of Materials (Ministry of Education), School of Material Science and Engineering, Northeastern University, Shenyang 110819, China; ruanlx948536015@yeah.net (L.R.); 1670523@stu.neu.edu.cn (X.Y.); qingw@smm.neu.edu.cn (G.Q.)
[2] Computer Teaching and Researching Section, Shenyang Conservatory of Music, Shenyang 110818, China; changyf537@126.com
[3] Suzhou Institute of Biomedical, Engineering and Technology, Chinese Academy of Sciences, Suzhou 215163, China; zhoulq@sibet.ac.cn
* Correspondence: zhangxm@atm.neu.edu.cn

Abstract: Poly(vinylidene fluoride), PVDF, as one of important polymeric materials with extensively scientific interests and technological applications, shows five crystalline polymorphs with α, β, γ, δ and ε phases obtained by different processing methods. Among them, β phase PVDF presents outstanding electrical characteristics including piezo-, pyro-and ferroelectric properties. These electroactive properties are increasingly important in applications such as energy storage, spin valve devices, biomedicine, sensors and smart scaffolds. This article discusses the basic knowledge and character methods for PVDF fabrication and provides an overview of recent advances on the phase modification and recent applications of the β phase PVDF are reported. This study may provide an insight for the development and utilization for β phase PVDF nanofilms in future electronics.

Keywords: β phase PVDF; electroactive properties; nanofilms; sensor and actuator; spin valve devices

1. Introduction

Poly(vinylidene fluoride), PVDF, with interesting scientific and technological properties is the typical representative of polymeric materials [1]. PVDF shows five crystalline polymorphs with α, β, γ, δ and ε phases depending on different processing methods [2,3]. Because of the antiparallel packing of the dipoles, the α and ε phases are non-polar [4]. The other three PVDF polymorphs are polar and show ferroelectric and piezoelectric properties. α, β and γ phases PVDF are mostly investigated for their properties and their extensive applications [5]. α phase PVDF is easy to obtain, which attracts wide interest to research melt crystallization of PVDF and α to β transformation [6]. Promoting β and γ phases in PVDF is an ongoing pursuit due to the most electrically active β and γ phases in the past studies [7,8]. Electroactive β and γ phases PVDF could be extensively utilized in spin valve devices, sensors, energy storage, etc. Moreover, the β phase PVDF was widely investigated for its interesting properties of the pyro-, piezo-, and ferroelectricity, and its inherent properties of light weight, mechanical flexibility, and easy processing. This paper mainly reviews the processing, properties and applications of the β phase PVDF.

2. Phases Characters of PVDF

The chain conformation for different phases of PVDF, respectively α, β and γ phases is shown in Figure 1. The α phase is the one commonly obtained directly from the melt by crystallization. The all-trans planar zigzag conformation of β phase can induce a significant dipole moment. Furthermore, a large

spontaneous polarization is generated by additive dipole moments. The piezoelectric effect of γ phase is weaker than β phase PVDF due to a gauche bond existed in every fourth repeat units [9]. So the β phase PVDF shows best piezo-, ferro- and pyroelectric properties among the five polymorphs of PVDF generally [10,11]. The lattice parameters of an orthorhombic β phase PVDF can be expressed as $a = 8.47$ Å, $b = 4.90$ Å, and $c = 2.56$ Å [12]. Three characterization methods, namely X-ray Diffraction (XRD), Fourier Transform Infrared Spectroscopy (FTIR), Differential Scanning Calorimetry (DSC) are used to study the formation and contribution of different crystalline phases of PVDF.
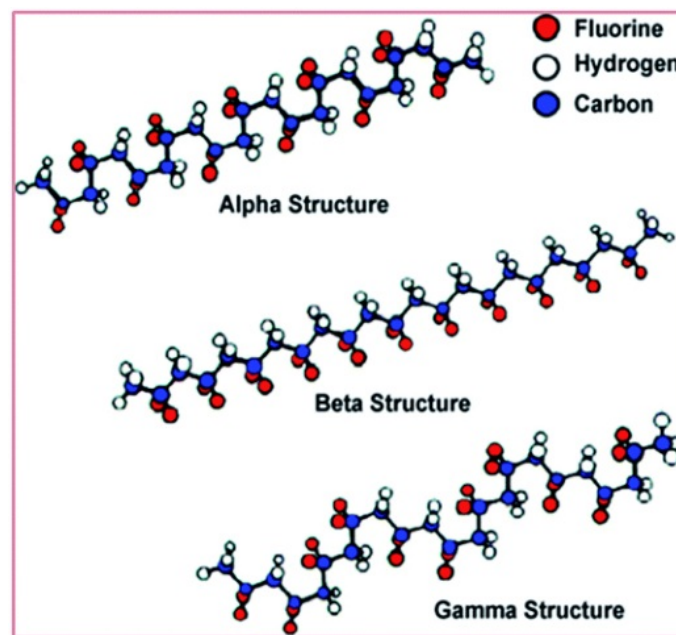
Figure 1. Diagrams of the chain conformation for α, β and γ crystalline phases of PVDF [13].

The XRD and FTIR can implement the qualitative identification and quantitative analysis of the β phase (Figure 2a,b). DSC is a thermo-analytical technique that has been complementary to the other identification techniques to identify the crystalline phase of PVDF. The XRD spectra (Figure 2a) confirm that the peaks at 17.7°, 18.3° and 19.9° characteristic of the α phase of PVDF, and the peaks at 18.5°, 19.2°, 20.0°, characteristic of the γ phase. The peak at $2\theta = 20.26°$ is related to the diffraction of β phase at (110) and (200) [14–16]. FTIR spectra of these three PVDF polymorphs have been investigated thoroughly and extensively [5,17–19]. Vibrational bands of α phase are at 530 cm^{-1}, 615 cm^{-1} and 765 cm^{-1} and 795 cm^{-1}, while vibrational bands exclusively of β phase are at 510 cm^{-1} and 840 cm^{-1}, and the bands correspond to the γ phase are at 431 cm^{-1}, 776 cm^{-1}, 812 cm^{-1}, 833 cm^{-1} and 1233 cm^{-1}, as shown in (Figure 2b). The melting temperatures of the β crystallites and α phase PVDF are similar at 167–172 °C (Figure 2c), so DSC is used to calculate the crystalline percentage, but not to distinguish these three phases [15,20]. As a result, two of the above three measurement techniques are needed to identify a specific phase at least.
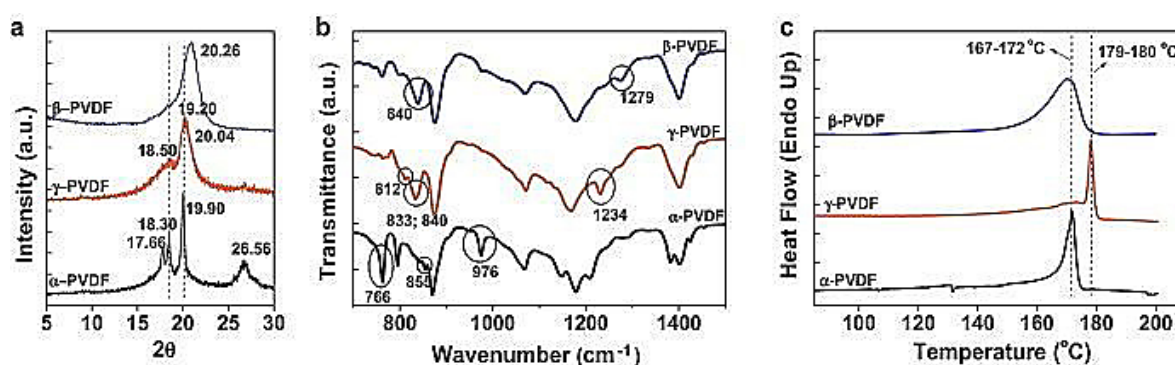
Figure 2. Synopsis of main experimental features of the different experimental techniques for correct identification of the PVDF phase: (**a**) XRD ($K_{\alpha 1,\gamma} = 1.5405600$ Å); (**b**) FTIR; and (**c**) DSC [16].

Though the IR spectrum of the α, β and γ phases includes many of the peaks due to overlapping absorptions, several unique peaks for different phases can be used for identification and quantification of the α, β and γ phases, such as their relative amounts. The IR absorption bands, characteristic of the α and β phases in each sample are at 766 cm^{-1} and 840 cm^{-1}, respectively. The fraction of β phase, F(β), can be calculated using Equation (1) explained by Gregorio, and the formula is as follows:

$$F(\beta) = \frac{X_\beta}{X_\alpha + X_\beta} = \frac{A_\beta}{(K_\beta / K_\alpha) A_\alpha + A_\beta} \tag{1}$$

where X_α and X_β in Equation (1) are representative for the mass fraction of α and β phases, absorption bands at 763 cm^{-1} and 840 cm^{-1} are represented by the A_α and A_β and the absorption coefficients are expressed by K_α and K_β at the particular wavenumber, respectively. This equation was used to quantify the FTIR results [5]. It is known that the peaks may be assigned to the different crystal phases. One issue is the overlapping of various peaks. The overlapping peaks could be deconvoluted using OMNIC software [21,22]. The aforementioned method can be used to calculate the crystalline phase content of PVDF when just two phases are present in the material (α and β, γ and β or α and γ).

3. Processing Techniques of β Phase PVDF

The β phase PVDF obtained by phase transitions, solvent casting, by the addition of nucleating fillers, or the development of PVDF copolymers have been researched extensively.

3.1. Phase Transition Methods

Phase transitions to obtain β phase PVDF can be divided into four methods depending on the processing conditions [23], as shown in Figure 3.

The β phase obtained from melt needs high pressure, high temperature, epitaxial growth on Kbr or other specific conditions [23,24], as shown line 1 in Figure 3. The high-pressure-crystallized PVDF including both the low-melting and high-melting phase was indicated in a detailed study [25,26]. Quenching and then annealing of the PVDF films can induce the crystallization of β phase directly from the melt in the very early study of Yang et al. [26]. The α phase PVDF has been obtained directly from the melt [17,27–30]. The α to β phase transformation of PVDF(see line 2 in Figure 3) through the stretching annealing or poling process [31]. The fabrication of β phase PVDF by uniaxial drawing of α form film shows a typical piezoelectric character, which was proposed firstly by Kawai in 1969 [32]. This transformation idea has been widely investigated at different temperatures, stretching rate and tensile elongation [33]. The α to β phase conversion can be realized below 100 °C stretching temperatures, and about 3–5 stretch ratio in many studies [4,29,34,35], and the thickness of the prepared β phase PVDF films can range between several μm to hundreds μm. The piezoelectric properties of mechanically drawn PVDF are much improved by high-pressure crystallization PVDF

film [36]. The maximum β phase (ca. 85%) could be achieved from α phase by Sharma et al. [37]. Strictly speaking, poling of PVDF films and fibers is done in order to obtain aligned β PVDF crystallites, and is in this sense not a method to induce the β phase. However, the β phase prepared by "drawing at low temperatures" is not piezoelectric due to the random orientation. The poling is needed to orient all β crystals into one direction to obtain a functional piezoelectric material [38]. Meanwhile, the transformation of α to β phase also occurs after poling with high electrical fields (100–400 mV/m) [39]. The γ phase is obtained near the melting point by annealing, or produced by casting method from dimethyl sulfoxide (DMSO), and δ phase can be obtained in strong electric fields by poling the α phase PVDF [40–42]. The γ to β phase transformation during uniaxial stretching is reasonable (see line 3 in Figure 3) because that of γ phase is a high energy intermediate between α and β phase (see line 3 in Figure 3). The γ phase can be transformed into β phase by poling at 120 °C, and the poled β PVDF films exhibit very strong and persistent piezoelectric effect up to 205 °C [36]. In addition, the δ phase can transform into β phase as shown line 4 in Figure 3 by poling at high electric field. The piezoelectric charge coefficient, d_{33}, of −36 pm/V for the δ phase via solid-state-processing was reported very recently [43]. Interestingly, this value notably higher than electroformed δ PVDF (−15 pm/V) may open a new range of the piezoelectric PVDF materials [43].
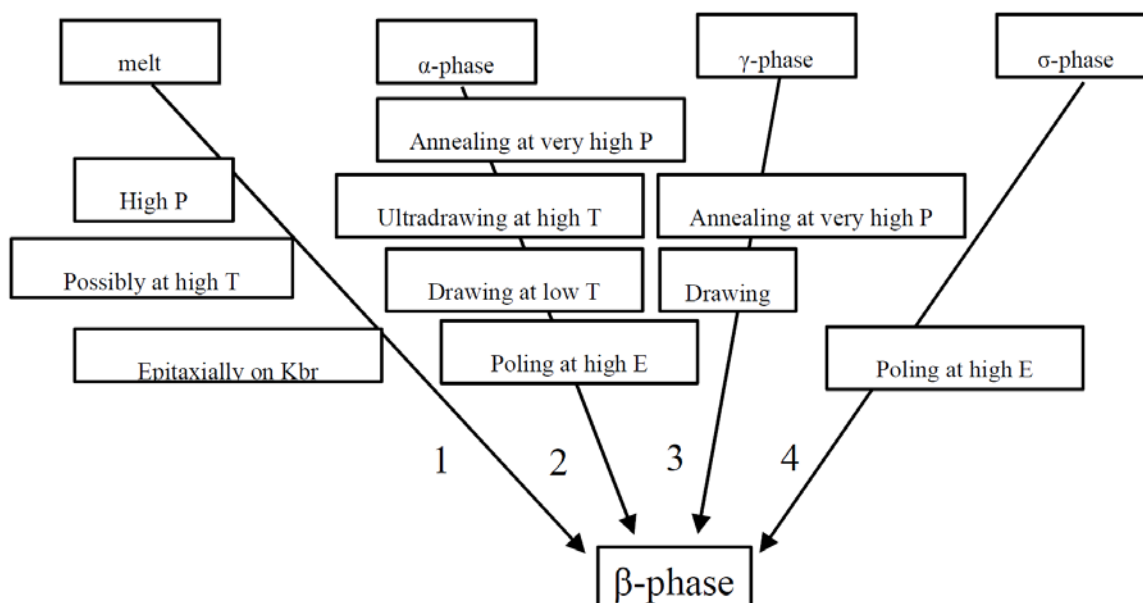
**Figure 3.** Four transition lines from different conformations to obtain β phase PVDF.

3.2. Solvent Casting

A variety of experimental technique with specialized conditions were explored to obtain the β phase PVDF from different conformations (e.g., epitaxial growth on alkali halide substrates [24], mechanical stretching of the conventionally prepared films [35], electrical poling [31], crystallization at high pressure [26], etc.). However, only films of well-ordered several μm thicknesses can be prepared, and free-standing films with nanoscale thickness is very hard to fabricate using most of these methods. nanoscale thickness PVDF films can realize many microelectronics applications when deposited on a suitable substrate [44]. Thus, researchers have paid more and more attention to develop more convenient methods to obtain nanoscale films and nanofibers of β phase PVDF from solvent casting methods, such as electrospinning, Langmuir–Blodgett, spin-coating and solvent evaporation. Solvent-cast films of PVDF in dimethyl formamide (DMF), dimethylacetamide (DMAC), and DMSO, have been reported to bring about the formation of β phase PVDF [5,45].

3.2.1. Electrospinning

Electrospinning technique has its superiority of versatility and consistency, much attention has been paid in the last decade to produce fibers in the submicron range using this method [46,47]. The β phase PVDF fibers can be formed from solution directly by electrospinning. This straightforward technique is relatively simple, fast, versatile and efficient. PVDF dissolved in DMF as electrospinning solutions has formed β phase PVDF nanofibers successfully in previous work [48–50]. The high ratio of stretching, which causes the α to β phase transition during the electrospinning is similar to the elongation during uniaxial mechanical stretching in some way.

PVDF fibers containing mainly β phase can be fabricated by control of the electrospinning conditional parameters such as electrospinning temperature, the solvent, the feeding rate, and distance between the tip and collector [51,52]. The fraction of β phase can reach 85% and the total crystalline fraction is higher than in the sample formed by the conventional methods we mentioned in the previous section in the work of Ribeiro et al. [46]. Figure 4 shows SEM micrographs of PVDF fibers directly produced from 20 wt. % PVDF solutions with different DMF/acetone ratios by electrospinning. The average fiber diameter was decreased with the increase of the DMF/acetone ratio and this phenomena can be interpreted to the higher boiling point and polarity of DMF than that of acetone [53]. PVDF fibers has attracted interest for various applications, including sensors, cell phones, batteries, biomedical applications, filtration, among others [54–56], and so many applications mean that the electrospinning technology for forming β phase PVDF fibers can achieve great development in the future.
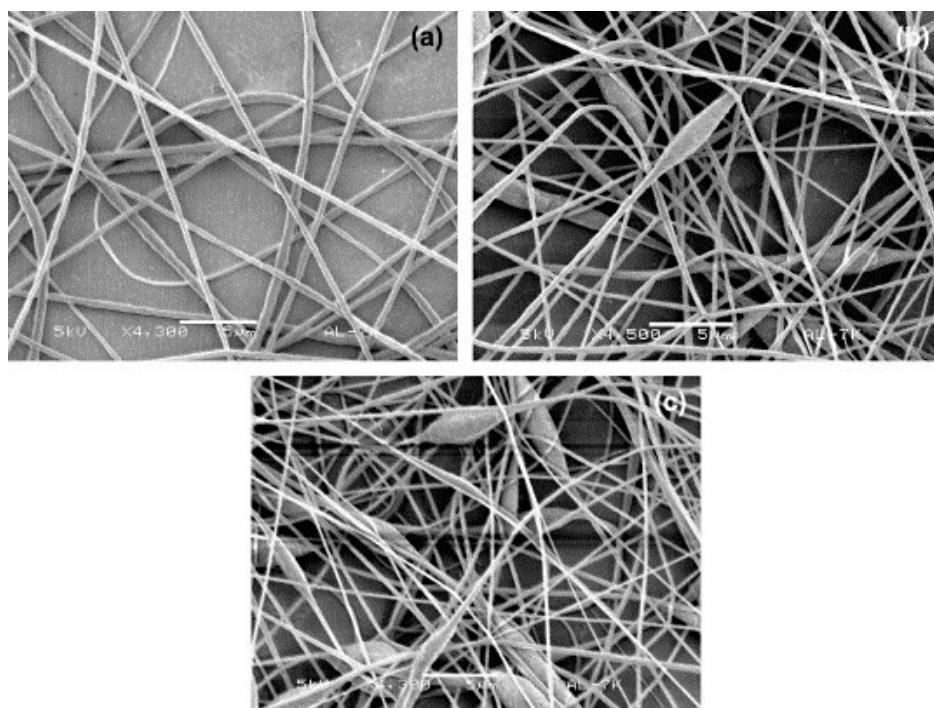
Figure 4. SEM micrographs of PVDF fibers obtained at 15 kV from 20 wt. % PVDF by electrospinning with different DMF/acetone weight ratios of: (**a**) 60/40; (**b**) 70/30; and (**c**) 80/20 [52].

3.2.2. Langmuir–Blodgett

Nanoscale films can be prepared by a monomolecular film assembly method, named the Langmuir–Blodgett (LB) technique [57]. Ferroelectric β phase PVDF is also formed directly during the LB deposition process. The forming of hydrogen bonds can result that the PVDF molecules on water surface are orientable with C–F groups, as illustrated in Figure 5, and a large value of effective

piezoelectric coefficient of PVDF LB film, -49.4 pm/V, was acquired in this research [58]. A few nanometers thick β phase PVDF, is fabricated by LB technique at 40 mN/m surface pressure using ultra-pure water as the subphase, and poling process is not necessary [59].
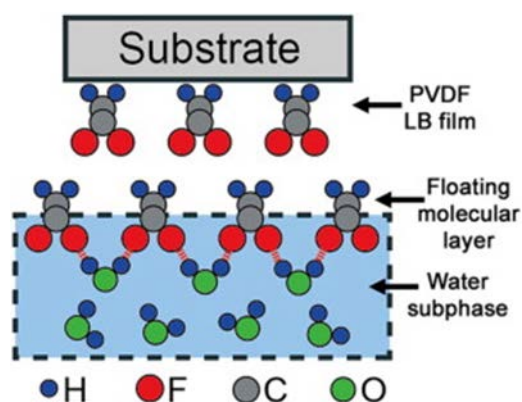
Figure 5. Schematic illustration of the oriented PVDF molecules and the subsequent transfer to form the LB film on a substrate [58].

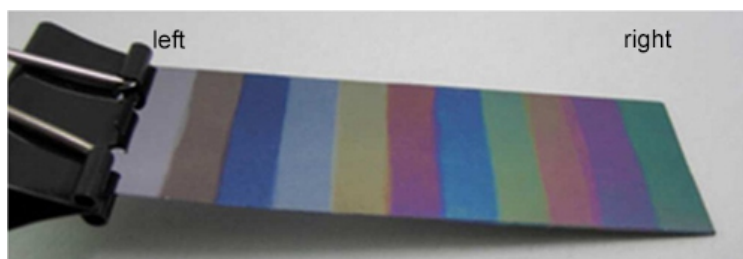The sequential deposition of single monolayer enables the symmetry of the film to be precisely defined [60,61]. The regular layer structure and the smooth film surface can be proved by the beautiful interference colors of different layers of PVDF LB nanofilms, a related photograph is shown in Figure 6.


Figure 6. PVDF LB nanofilms with different layers, from 0 (**left**) to 200 (**right**) layers [61].

Zhu et al. [62] prepared highly oriented ferroelectric PVDF LB nanofilms by an assistance of amphiphilic nanosheets. PVDF films with thicknesses of several nanometers was prepared by LB technique [63], and the almost 100% β phase PVDF films could be fabricated and simultaneously the monolayer thickness can be controlled by a 2 nm through monolayer transfer [64].

3.2.3. Spin-Coating

A thin, uniform polymer film can be produced from dilute solution on a planar substrate by a common method, known as spin-coating. Nanoscale films of β crystalline phase PVDF were directly obtained by heat-controlled spin coating [8,65,66]. Moreover, the spin-coating method is considered suitable to fabricate smooth polymeric coatings on an industrial scale for the microelectronics applications [8]. Benz et al. [45] prepared 2 μm thick PVDF films by spin coating PVDF solutions on single-crystal silicon wafers with acetone/DMF as a solvent. The main factors including humidity conditions and spin speed can determine the surface roughness of the thin films and the content of β phase. Cardoso et al. [67] demonstrate a simple and reproducible method to prepare electroactive β phase PVDF samples with the thickness controlled from 300 nm to 4.5 μm, and d_{33} from 0 to -21 pC/N with the electroactive phase content from 0 to 100%.

In our work, 3 wt. % PVDF was dissolved in DMAc solution and coated on ITO substrates to prepare ferroelectric PVDF film successfully using a heat-controlled spin-coating setup [65]. The microstructure and micropattern of the PVDF film obtained by spin coating method can be found in Figure 7, and the ferroelectric phase of PVDF film fabricated by spin coating combined with treatment was maintained up to 160 °C [8]. The dense β phase dominant PVDF film can be obtained on silicon substrates by spin coating with addition of hydrate salt [68]. The apparent longitudinal d_{33} was −17.4 pm/V and the remnant polarization was 69.5 mC/m^2.
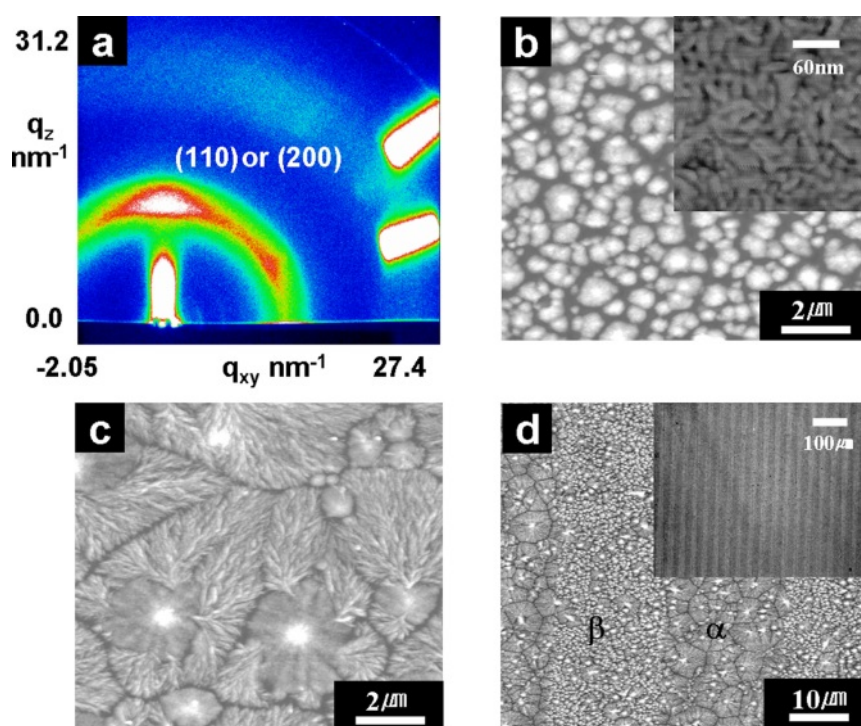
Figure 7. (**a**) 2D GIXD pattern and (**b**) AFM image of PVDF film with a 200 nm thick fabricated by spin coating on Au substrate and rapidly annealed at 150 °C; (**c**) AFM images of a PVDF film spin coating on treated Au substrate and rapidly annealed; (**d**) AFM image of αand βphase PVDF crystals [8].

3.2.4. Solvent Evaporation

The β phase thin films can be prepared by thermal evaporative deposition methods [69–71]. However, the thermal decomposition of the PVDF molecular chains seriously reduced the extent of ferroelectric response. Therefore, the solution deposition methods have been a possible use instead of the evaporative deposition [72–75]. Many reports have proved that the solution processing can produce devices based on silicon at significantly lower cost than conventional methods. The β phase obtained by solution trends to present a high porosity and an opaque appearance leads to a decrease of the electrical and mechanical properties. The pores in original sample can be eliminated after applying pressure perpendicular to the surface of β phase film at 60 °C at elevated temperature [74]. Oriented β phase films were obtained by drawing exclusively β phase films with subsequent pressing at 60 °C from DMF solution [75].

3.3. Copolymers

A wide variety of copolymers have been synthesized by incorporation PVDF with the trifluoro ethylene (TrFE), hexafluoropropylene (HEP) comonomer, chlorotrifluoroethylene (CTFE) or other polymers. The β crystalline phase of PVDF has been detected in the poly(tert-butyl methacrylate)-block-PVDF-block-poly(tert-butyl methacrylate) triblock copolymers [76]. The change

from α crystalline phase to the β crystalline phase was also confirmed by FTIR and XRD measurements in the block copolymers [77]. The development of poly(vinylidene fluoride-trifluoro ethylene) P(VDF-TrFE) has verified that the material obtained can possess the electroactive property. This copolymer also shows the Curie Temperature (T_c) lower than the melting temperature (T_m), and, in this way, allows the study of ferroelectric (FE) to paraelectric (PE) phase transition [78,79].

Ohigashi et al. [80] prepared "single crystalline films" of ferroelectric P(VDF-TrFE) (75/25 molar ratio) with the 5–100 μm thickness successfully in 1995. Poly(vinylidene fluoride-co-hexafluoro propene), P(VDF-HFP) has been mainly studied for applications on the area of polymer electrolytes, such as using in rechargeable lithium batteries and for the production of membranes for organophilic pervaporation [81,82]. PVDF has also been modified by the introduction of chloride trifluoride ethylene (CTFE) on the polymer chain, producing the P(VDF-CTFE) copolymer. The bulky CTFE can induce the structure of copolymer loose, which can make the orientation of dipoles easier under external electric field. The piezoelectric constant, d_{33} for this copolymer can reach the value of 140 pC/N [83,84].

3.4. Composites: Inclusion of Fillers within the Polymer Matrix

The β phase PVDF has been obtained by the addition of $BaTiO_3$ [85,86], clay [87], hydrated ionic salt [45], PMMA [88], TiO_2 [89], $CoFe_2O_4$ [90] or nanoparticles such as palladium, ferrite or gold [91] as nucleating fillers. It is also reported that β phase PVDF nanocomposites can be fabricated with the assistantance of ionic liquid [92,93].

The direct nucleation of the β phase PVDF can save processing some steps if the material obtained by extrusion processes and micro technology compatible technologies in the desired size and shape. The presence of $BaTiO_3$ can make β PVDF phase nucleate, and the nucleation is dependent on filler size strongly [86]. Martins et al. [94] prepared PVDF/ferrite nanocomposite by addition $NiFe_2O_4$ of and $CoFe_2O_4$ nanoparticles to nucleate electroactive β phase PVDF for multiferroic and magnetoelectric applications, and 50 wt. % of $NiFe_2O_4$ and 5 wt. % of $CoFe_2O_4$ can guarantee to obtain more than 90% β crystalline phase. They found the content of β phase increases with the increasing concentration of $CoFe_2O_4$ and $NiFe_2O_4$ in a different way in the following year [95]. The negative electrostatic charge of nanoparticles is used to elucidate the nucleation of β phase. The CH_2 bonds of the PVDF and the negatively charged ferrites surface have a strong interaction, which induces an extended TTTT conformation aligned on the surface of nanoparticles and results in crystallographic phase formation of the β phase PVDF.

4. The Electroactive Properties of the β Phase PVDF

The piezoelectric property of PVDF was first found by Kawai in 1969 [32], and the pyroelectric property of PVDF was found by Bergman et al. [96] and by Nakamura and Wada [97] two years later. PVDF has been investigated widely because of its pyro-, piezo- and ferroelectric effect within the last decades [98].

4.1. Piezoelectric Effect

A Mach–Zehnder interferometer was used to measure the sample strain for the measurement of piezoelectric property [99]. The piezoelectric coefficient d_{33} can be defined by Equation (2), and the strain was induced by the applied electric field.

$$d_{33}^T = \left(\frac{\partial S_3}{\partial E_3} \right)_T \tag{2}$$

where the strain S is caused by the external electric field E, and T is the constant stress. The direction of spontaneous polarization is along the x_3 axis. The three-dimensional tensor d_{ijk} is represented by two-dimensional d_{il}, where l represents the six different combinations of the indices (j, k). Figure 8

shows the d_{33} values increasing with the β phase content of samples, and both of them increase with increasing stretching ratios at 80 °C [100].
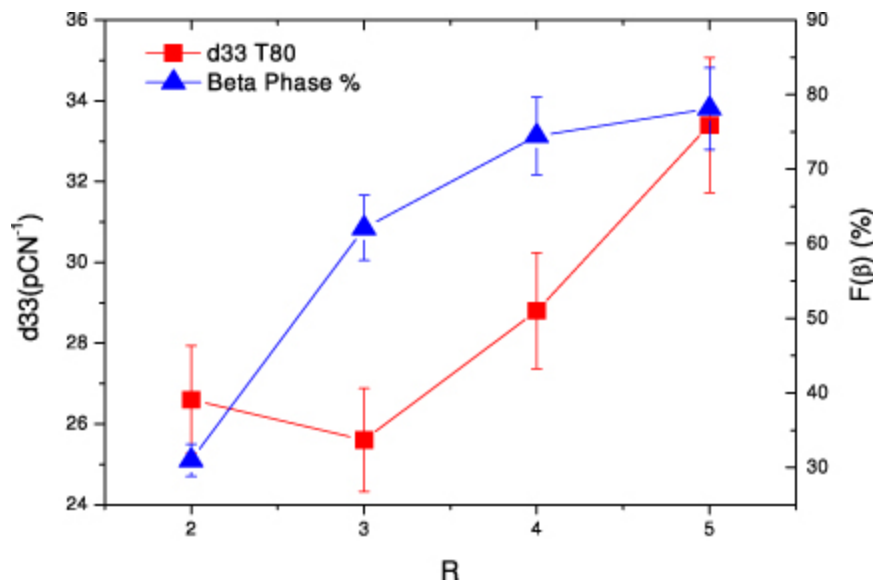
Figure 8. d_{33} and F(β) (%) for samples depending on stretching ratios R at 80 °C [100].

The decreasing d_{33} of PVDF indicated that thermal depoling can be caused by annealing at an elevated temperature. The polymer retains 32% of its original d_{33} value after annealing at 140 °C. The decrease of d_{33} may also orginate from the random orientation of β phase PVDF. So thermal poling could orient all beta-crystals into the same direction [101]. (CH$_2$-CF$_2$)$_n$ is the chemical structure of PVDF molecules, and after poling the CF$_2$ dipoles are aligned normal to the surface of the film and form a residual polarization. The C_{2v} (2 mm) represents the symmetry of poled films, if the z axis is assigned normal to the surface of films in the poling direction, the x axis along with the direction of elongation, and perpendicular to the x and z axes can confirm the y axis. Five piezoelectric coefficient observed values are $d_{31} = 20$ pCN^{-1}, $d_{32} = 1.5$ pCN^{-1}, $d_{33} = -32$ pCN^{-1}, $d_{15} = -27$ pCN^{-1}, and $d_{24} = -23$ pCN^{-1}, are finite, respectively [102].

4.2. Pyroelectric Effect

Pyroelectric effect is defined as the spontaneous polarization depended on the temperature of certain anisotropic solids [103]. In principle, there are two ways that the pyroelectric coefficient can be measured: either by holding the size and shape of the sample constant while the temperature is changed or by allowing the sample to expand and change shape freely as a result of thermal expansion. In the second experiment there is an secondary pyroelectricity resulting from piezoelectricity [104]. Pyroelectric measurements can be implemented by using both slow heating/cooling method and Chynoweth method [105,106]. The different thermal expansion coefficient between the substrate and the polymer makes the film expand and contract just perpendicular to the surface, so two contributions are included in the measured pyroelectric coefficient $p_3(eff)$ in Equation (3), namely the primary and the secondary effect: [107]

$$p_3(eff) = \left(\frac{\partial P_S}{\partial T}\right)_S + \frac{d_{33}^T \alpha_3^S}{S_{33}^S} = \left(\frac{I}{A}\right)\left(\frac{\partial T}{\partial t}\right)^{-1} \tag{3}$$

where $p_3(eff)$ is the pyroelectric coefficient, S is the strain, T is temperature, d_{33}^T is the stress-free piezoelectric coefficient, α_3^S is the thermal expansion coefficient, S_{33}^S is the elastic compliance coefficient,

A is the surface area, the pyroelectric current is represented by *I*, and the rate of temperature change is expressed by $\partial T/\partial t$. The temperature was controlled by a microprocessor [99]. Figure 9 shows that the pyroelectric coefficients (*P*) are depended on the heating rate, concentration of BaZrO₃, and temperature [108].
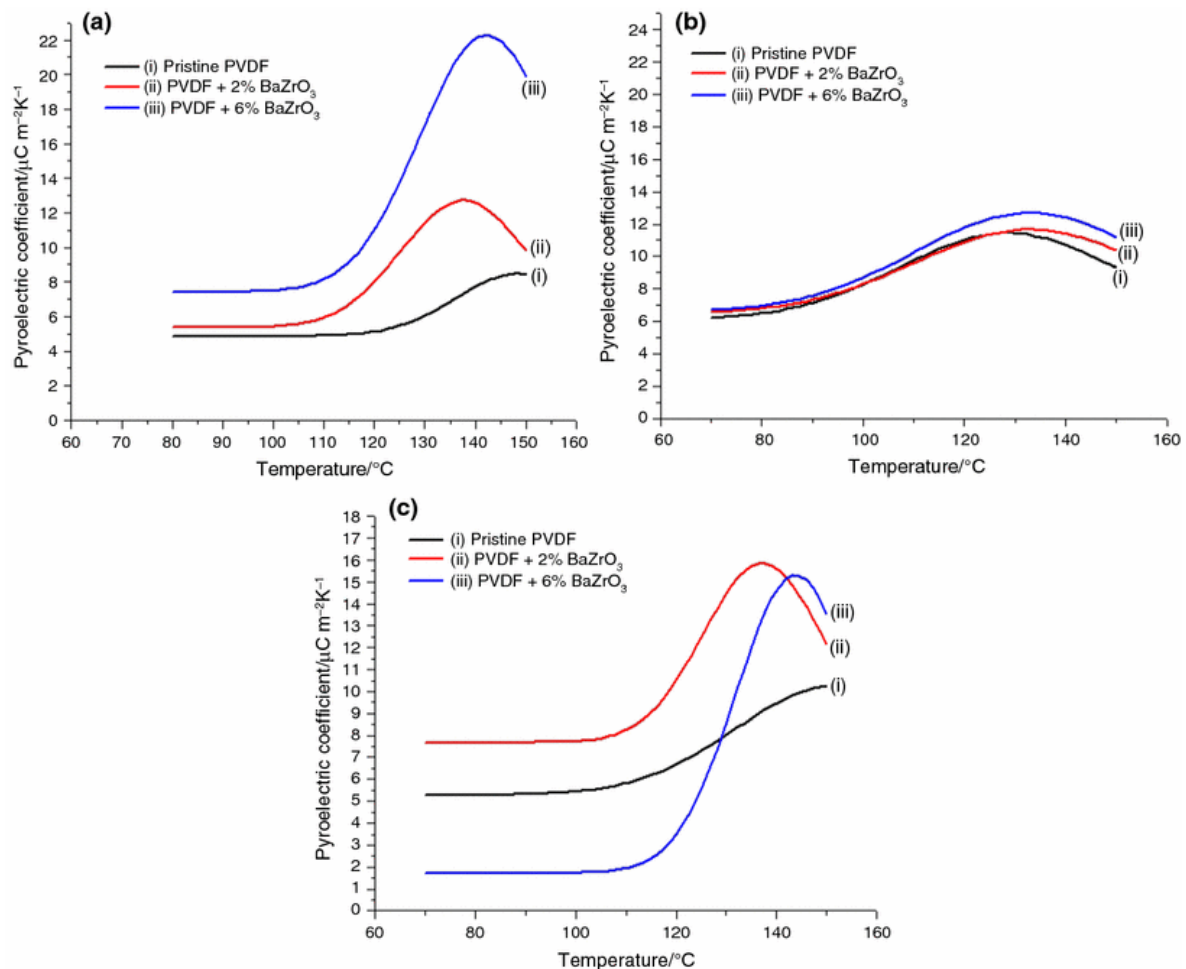
Figure 9. Pyroelectric coefficient of PVDF and PVDF nanocomposites depended on temperature of (**a**) 1 °C/min, (**b**) 2 °C/min, and (**c**) 3 °C/min heating rate [108].

4.3. Ferroelectric Effect

The ferroelectric property of PVDF was anticipated since the large piezoelectric effect was reported for PVDF. In 1974, the observation of the hysteresis loop was successfully performed [80]. PVDF has extremely potential to be used in multi-functional MR devices as an organic ferroelectric material. A previous study has shown that the D-E hysteresis loop of PVDF is independent on the frequency of the applied field between 10^{-2} and 10^{-4} Hz at room temperature [109]. The D-E hysteresis loops are shown in Figure 10a, and the remanent polarization (P_r) and coercive field (E_c) dependent of the different film thicknesses of PVDF LB nanofilms are shown in Figure 10b. A P_r of 6.6 µC/cm² for PVDF nanofilm with 81 nm thickness was obtained without post-treatment, and ferroelectricity was detected first in a PVDF nanofilm with 12 nm thickness, indicating a potential application of PVDF films at low-voltage [110].

The ferroelectric effect of PVDF originates from the dipole moments in the PVDF molecule. The dipole moments stem primarily from the presence of fluorine atoms which have the strongly electronegative [111,112]. The PVDF thin films fabricated from the melt or a solution have no

ferroelectric effect because the dipole moments cancel in the crystal structure and stereo-chemical conformation, additional steps such as stretching, using P(VDF-TrFE) instead of PVDF are needed to make these films ferroelectric [113]. Ferroelectricity has many features similar to ferromagnetism including a shift of the phase transition temperature $T_c(E)$ with applied electric field and the disappearance of the spontaneous polarization above the zero-field Curie point T_{c0} [107]. In this following report, we will mainly discuss the applications of β phase PVDF. Other studies about PVDF with various phases can be found in the literatures [114–127]. These investigations would also be very useful for future applications.
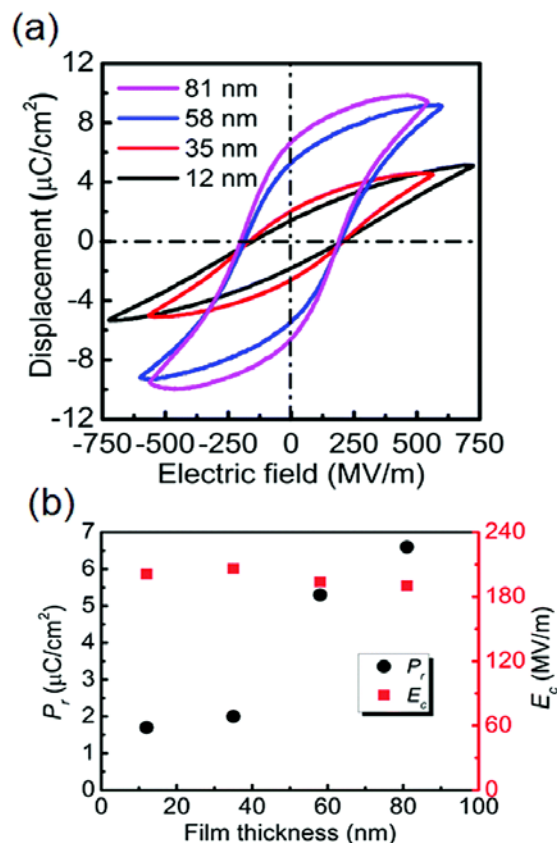
Figure 10. (**a**) The D-E Hysteresis loops and (**b**) coercive field (E_c) and remanent polarization (P_r) of PVDF nanofilms dependent of different film thicknesses [110].

5. Applications of the β Phase PVDF

Kawai found the tensile piezoelectricity of PVDF in stretched and poled films in 1969 [32]. In addition, then PVDF have many applications as ultrasonic transducers, batteries, actuators, chemical warfare protection, magnetoelectric, filters, and in the biological fields.

In 1972, ultrasonic transducers making use of the piezoelectric constant d_{33} of PVDF, were first produced. Electroacoustic transducers utilizing the piezoelectric constant d_{31} of PVDF, were marketed in 1975 [128]. The cell response and fibronectin adsorption on electroactive PVDF films make PVDF possible to be active substrates [129]. Various applications of PVDF and its copolymers have been greatly developed during almost five decades. Here we chose several promising applications which were widely concerned by researchers recently to introduce.

5.1. Sensor and Actuator Applications

Actuators have potential applications and attracted much attention in recent years because the sensor can convert a mechanical variable into a measurable electrical quantity. PVDF has been quite

extensively applied in sensing and actuator due to its inherent piezoelectric effect. The applications of Actuator based on PVDF can be found in acoustic emission monitoring, controlled displays, robots and artificial muscles [130–133], and a series of studies have been done to explore the use of PVDF such as weight, pressure sensor [134–139]. Active vibration control by a laminated PVDF actuator is studied [132], and an SGO/PVDF bilayer actuator can respond to moisture, light and heat with excellent stability and repeatability [140]. The PVDF/graphene actuators show faster response time and larger bending deformation than the pure PVDF actuator [141]. Fully plastic actuator through layer-by-layer casting with ionic-liquid-based bucky gel was reported by Takanori et al. [142]. They also proposed a new two-step process for preparing a gelatinous mixture composed of the SWNTs. In this study, the ionic liquids and PVDF-HFP as a polymer support improved the performance of the actuator [143].

A PVDF film microforce sensor was designed and fabricated to measure the strength of fiber bonds successfully, and this microforce sensor is able to measure the forces up to 10 mN [144]. Choi et al. [145] use macro fiber composite actuators and PVDF sensors to enhance the damping performance of the rotating composite thin-walled beam. A quartz crystal microbalance modified by PVDF was used to detect the dimethyl methyl phosphonate (DMMP) vapor [146]. Highly sensitive, wearable and wireless pressure sensor successfully fabricated based on the zinc oxide (ZnO) nanoneedle/PVDF hybrid film was shown in Figure 11.
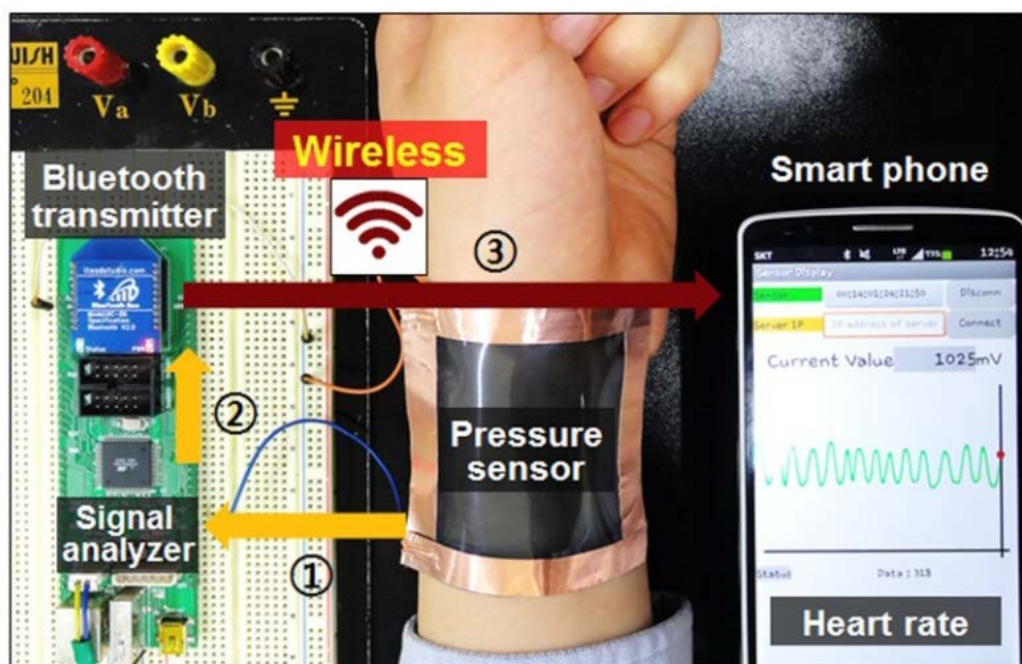
Figure 11. Photograph of wearable and wireless pressure sensor for heart rate monitoring [147].

Kim et al. make a significant contribution to fabricate sensors based on PVDF fabrics [148]. Several factors should be taken into account in fabrication of the force sensors, such as electrospinning parameters, fiber alignments, and materials of the electrodes [149]. The addition of nanofillers can increase the β phase PVDF commonly in composites, and in turn can improve the piezoelectric response for sensor and actuator applications [150,151]. A highly sensitive tactile sensor based on an Organic Charge Modulated FET (OCMFET) and PVDF has been reported by Spanu et al. [152]. The structure of the sensor can be found in Figure 12a, and the output and input characteristics for pressure sensing was shown in Figure 12b. This proposed device can transduce applied pressure as low as 300 Pa range with good reliability in a wide frequency, opening the possibility to fabricate tactile transducers with highly sensitive using large area fabrication techniques.
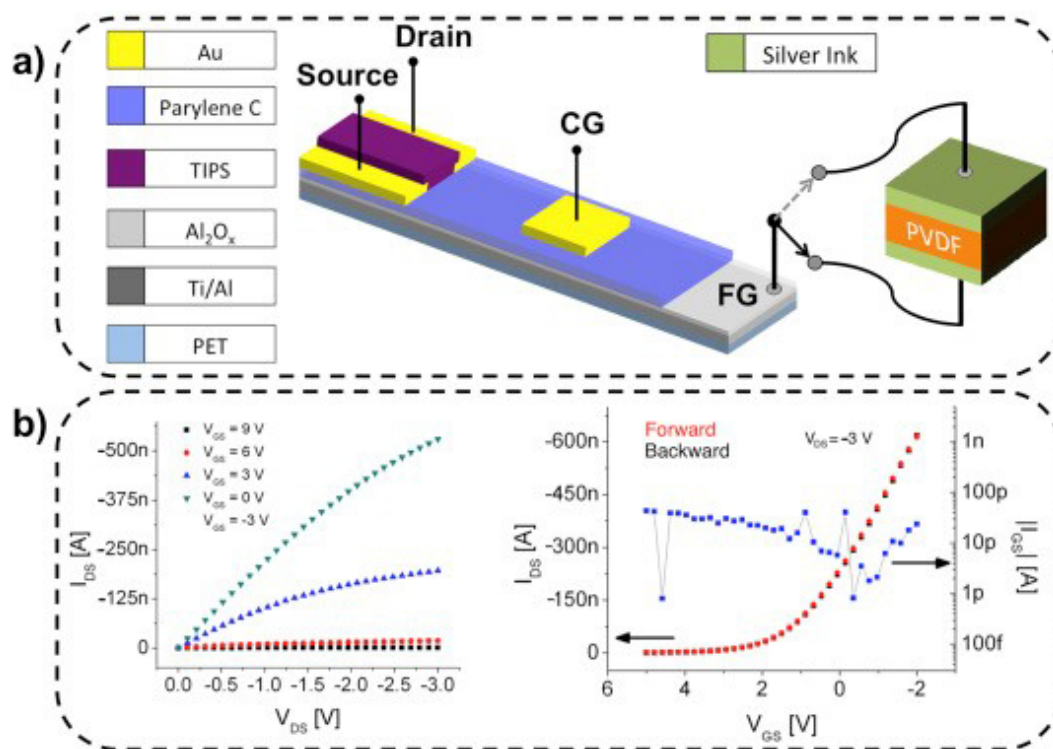
Figure 12. (**a**) The designed structure of the highly sensitive tactile sensor and (**b**) Output and input characteristics of designed device for pressure sensing [152].

5.2. Spin Valve Devices

Various organic ferroelectric materials have existed, but much attention is focused on PVDF and its copolymer due to its several advantageous properties including short switching time, relatively large remnant polarization, and good thermal stability [113].

Many efforts are paid to fabricate nonvolatile and rewritable memory devices using organic PVDF. Memory devices utilize the hysteresis by associating the polarization states to form the basis for most logic circuits. Some of these efforts are focused on metal/organic semiconductor/metal junctions [153], field-effect transistors [154], and switches [155]. PVDF and P(VDF-TrFE) can be placed between the capacitor electrodes as the ferroelectric medium [111]. Ferroelectric PVDF switching has an activated process depending on not only the temperature, but the applied field strength. $La_{0.6}Sr_{0.4}MnO_3$/PVDF/Co.-based multiferroic tunnel junctions shows a tunable spin polarization at the PVDF/Co. interface depending on the ferroelectric polarization of PVDF. Remarkably, a change of tunneling magneto-resistance sign found when the PVDF polarization is reversed can be explained by the ferroelectric change of spin-polarization in the second PVDF layer close to PVDF/Co. interface, which acts as an efficient spin-filter for electron tunneling through PVDF barrier [156]. Ferroelectric PVDF have been used to fabricate magnetoresistance (MR) devices as spacer layers at low temperatures. The β phase PVDF films were fabricated by the LB technique and then used to prepare the organic spin valve devices successfully (Figure 13a) by Zhang et al. [64]. It is valuable using PVDF for multi-configuration spin control to fabricate future flexible spin devices, more than that, they have achieved an MR ratio over 2.5% at room temperature for the PVDF spin devices (Figure 13b).
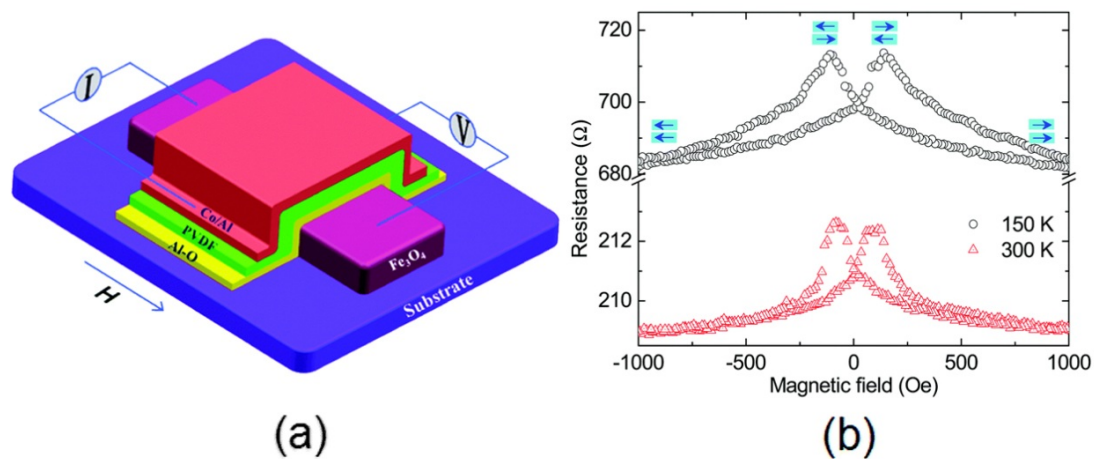
Figure 13. (**a**) Schematic diagram of the spin valve device with an Fe_3O_4/AlO/PVDF/Co./Al stacking structure; and (**b**) Magnetoresistance curves for the device at 300 K (red triangles) and 150 K (black circles) [64].

Furthermore, Zhu et al. [62] report a PVDF ferroelectric nanocapacitor which shows asymmetric hysteresis loops, and it results in different remnant polarization values of -15 μC/cm^2 for $-P_r$ and 6.0 μC/cm^2 for $+P_r$. This peculiar discovery opens up the probable applications of ferroelectric PVDF for the diode.

5.3. Magnetoelectric Materials

The induced magnetization by an applied electric field variation as well as the electrical polarization of a material in the presence of an applied magnetic field can be defined as magnetoelectric (ME) effect [157–159]. The magnetoelectric (ME) effect is the bridge between the electric properties and magnetic properties of materials. A strong ME effect at room temperature is generally obtained by combining piezoelectric and magnetostrictive components [160]. ME materials using piezoelectric polymers appear to be very suitable due to their versatility of production, flexibility, and low cost [161]. The magnetoelectric materials can be distinguished from other materials in Figure 14a. Polymer-based ME materials are an innovative, challenging and interesting research field, which should bridge the gap between fundamental research and practical applications. Laminated composites, nanocomposites and polymer as a binder composites are the three types of polymer-based ME materials [159]. The ME materials have immensely potential applications in numerous areas such as spintronics, multiple-state memories, actuators, transformers, information storage, sensors, diodes, among others [162–166]. The bilayer PVDF/Metglas laminates magnetic sensors for detection of weak dc magnetic field shows quite high sensitivity [160]. The ME laminates consisting of Metglas/PVDF unimorph has been studied and shows an excellent sensitivity to small variations in both ac and dc magnetic fields [167]. Furthermore, the energy-harvesting applications using polymer-based ME composites have recently been proposed by harvesting energy from wind, sun, electromagnetism, etc. [159,168]. An energy-harvesting device was designed using PVDF as the piezoelectric element and $Fe_{64}Co_{17}Si_7B_{12}$ as amorphous magnetostrictive ribbons [169].
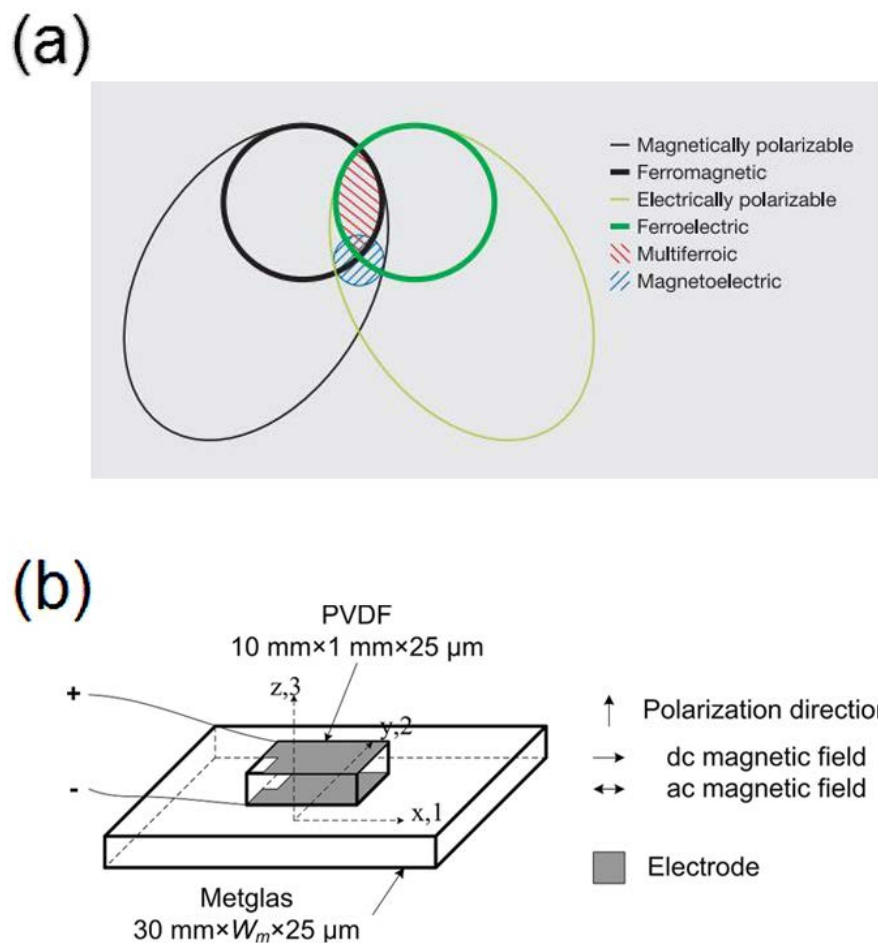
Figure 14. (**a**) The relationship between multiferroic and magnetoelectric materials [157] and (**b**) Diagrammatic sketch of Metglas/PVDF composite laminates [170].

Intensive works and more attention are devoted to ME material after the first report on Metglas/PVDF laminate nanocomposites [167]. Schematic diagram of Metglas/PVDF composite laminates was showed in Figure 14b. The sheet aspect ratio values of α_{31} = 21.46 V cm^{-1} Oe^{-1} were obtained in the PVDF/Metglas laminate at 3 Oe DC magnetic field and a frequency of 20 Hz [170]. A flexible planar structure of amorphous ferromagnetic Metglas—piezopolymer PVDF, and the ME coefficient was estimated as $\alpha_E = u/(bh) \approx 0.47$ V/(cm·Oe) at optimum bias field Hm [171]. The composite laminates of PVDF and the magnetostrictive layer have the strong coupling effect, which can induce large ME coupling coefficients at room temperature and have attract much attention of researchers [159,167,170–173].

5.4. Energy Harvesting Applications

Energy harvesting applications of piezoelectric and pyroelectric PVDF are developed rapidly which concentrate on devices, including 'nanogenerators' [174], nanoscale materials and various potential devices. This includes the conversion of mechanical vibrations to electrical energy via piezoelectric effect and the convert thermal fluctuations into electrical energy by pyroelectric effect [13,175–177]. The hybrid systems for harvest energy from multiple sources is possible since piezoelectric effect and pyroelectric effect are always present simultaneously. Figure 15 shows a flexible nanogenerator (NG) fabricated with a PVDF film [178]. Flexible piezoelectric nanogenerators were fabricated based on BaTi$_{(1-x)}$Zr$_x$O$_3$ and a PVDF polymer matrix using an ultrasonication probe process [179].
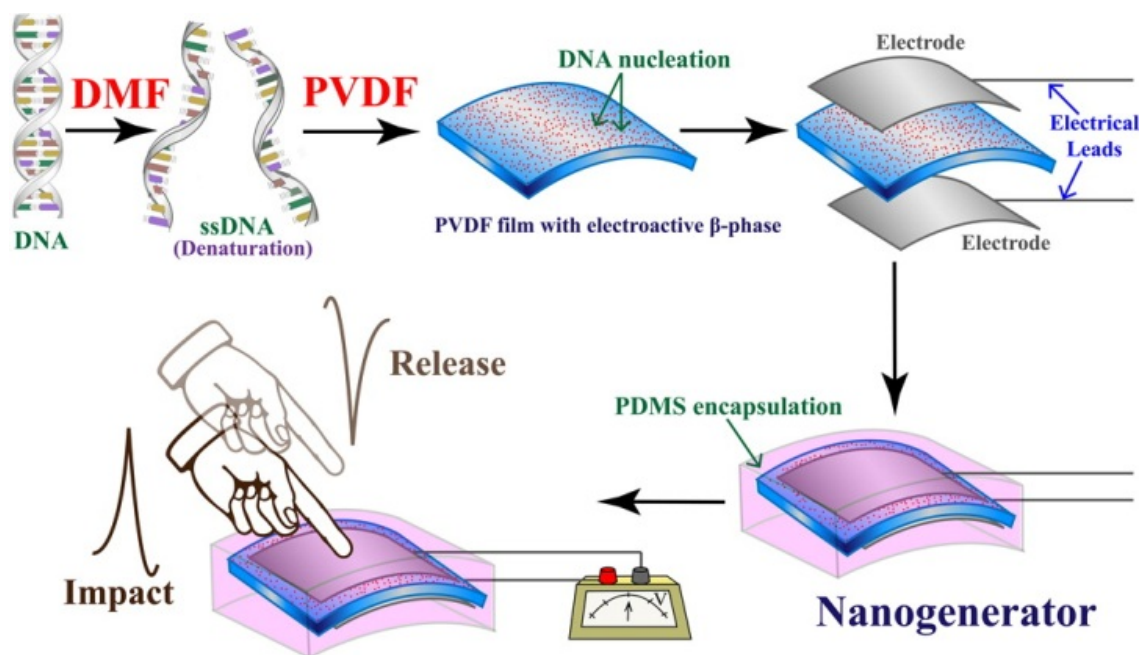
Figure 15. The structure of a flexible nanogenerator for Portable Electronic Devices [178].

A novel energy harvesting backpack using PVDF was developed that can generate electrical energy from the differential forces between the backpack and the wearer by Farinholt et al. [180]. An energy harvesting comparison of PVDF and ionic polymer transducer was proposed [181]. Sun et al. [182] reported that the PVDF microbelts can offer sufficient electrical energy for small electronic devices. Li et al. [183] reported a Bi-resonant structure with PVDF film for piezoelectric energy harvesting, which can improve the conversion efficiency from vibration to electricity by 40–81% significantly. The piezoelectric coefficients of its copolymers are larger than PVDF such as PVDF-TrFE ($d_{31} \cong 25$ pC/N and $d_{33} \cong -30$ to -40 pC/N) [184]. So many copolymers have been previously investigated for energy harvesting application. A flexible piezoelectric nanogenerator based on PVDF-TrFE thin film was fabricated, and it can exhibit reasonable electrical outputs and good stability [185]. Lallart et al. [186] evaluated the energy scavenging abilities using electrostrictive polymer P(VDF-TrFE-CFE), and they extended their work to make the practical application more realistic by researching the ac-dc conversion for energy harvesting [187].

5.5. Tissue Engineering

The piezoelectric properties of living tissue have been also reported and PVDF as a piezoelectric material has attracted more attention in tissue engineering research [188]. Piezoelectricity can be found in different parts of the human body, such as bone, ligaments, etc. [189–193]. Tissue engineering has emerged for tissue repair and regeneration as an alternative method, as presented in Figure 16a. Figure 16b shows one promising strategy to repair or regenerate damaged bone.

Young et al. fabricated microporous PVDF membranes for nerve tissue engineering by immobilizing L-lysine covalently on the surface of PVDF membrane [194]. The collagen from non-mammalian sources could be used to confer bioactivity to PVDF with hemocompatibility to bovine collagen and comparable cell-material interactions [195]. Therefore, the tissue engineering strategies based on PVDF materials show potential applications for human health.
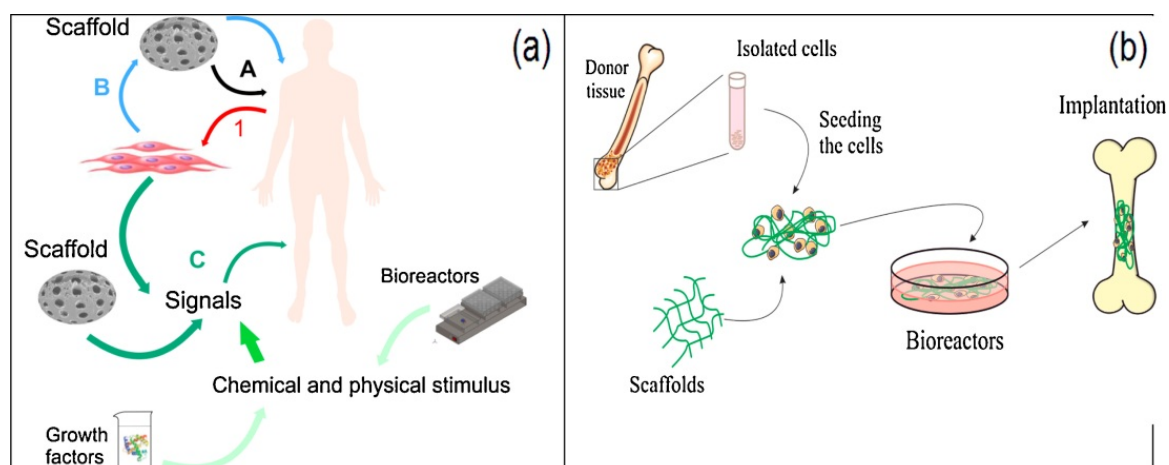
Figure 16. (**a**) Schematic diagram of the different strategies in the tissue engineering field: 1—the cells harvested directly from the patient; A—scaffold implanted directly; B—cells cultured in scaffold and then implanted; C—cells cultured in scaffold with appropriate signal and then implanted. (**b**) Tissue engineering strategies for bone regeneration [192].

5.6. Modelling Studies for PVDF

Modelling work for PVDF has been performed and the results are very interesting [196–199]. The atomistic modelling can be used to understand the changes at a molecular level on account of the poling process [39]. Holman and Kavarnos reported that the increase of both the trans bond number and structural order in P(VDF-TrFE) during the cooling process from the melt [200]. Bóhlen and coworkers have proven copolymerization of VDF with TrFE can form the all-trans PVDF conformations [197]. Moreover, the adhesion of single wall carbon nanotubes and the PVDF can be studied by molecular dynamics calculations [201]. In addition, They also proposed that the combination of atomistic simulations and macro-scale experiments could study the torsion angle distribution of PVDF in the melt [202]. The first-principles methods were also used to investigate the PVDF spin devices [203,204]. Their results indicate that β phase PVDF has enormous potential in organic spintronics for nonvolatile data storage and low-power electronics.

5.7. Reversible 3D Shape Transformation of the PVDF Film

The materials capable to translate the environmental stimuli into desirable shape changes have a bright prospects in emerging fields such as soft robotics, sensors, energy harvesting, multifunctional bio-scaffolds and metamaterials [205,206]. Responsive shape changes of a porous polymer film driven by gradients of electrostatic complexation have been reported recently [207]. Responsive shape changes of a carbon nitride polymer film actuated by anisotropic crystalline orders was reported more recently [208].

Very recently Deng et al. [209] report a new responsive film which possesses an anisotropic spatial distribution of the α and β phase PVDF, and this PVDF film can response to organic vapors in high sensitivity and a fast response rate. The crystal phase anisotropy can be programmed easily in different directions and locations of the PVDF films by a direct laser writing technique (Figure 17a). Experimental and simulation results show the shape change is attributed to the distinct absorption abilities for acetone between α and β phase PVDF. Many complex structures can be obtained by different folding creases on the PVDF films, including a complex shape transformation from 2D to 3D (Figure 17b–f). This responsive shape change will inspire researchers to explore more polymeric materials and further investigate for the underlying applications in artificial muscles, soft robotics sensors, etc.
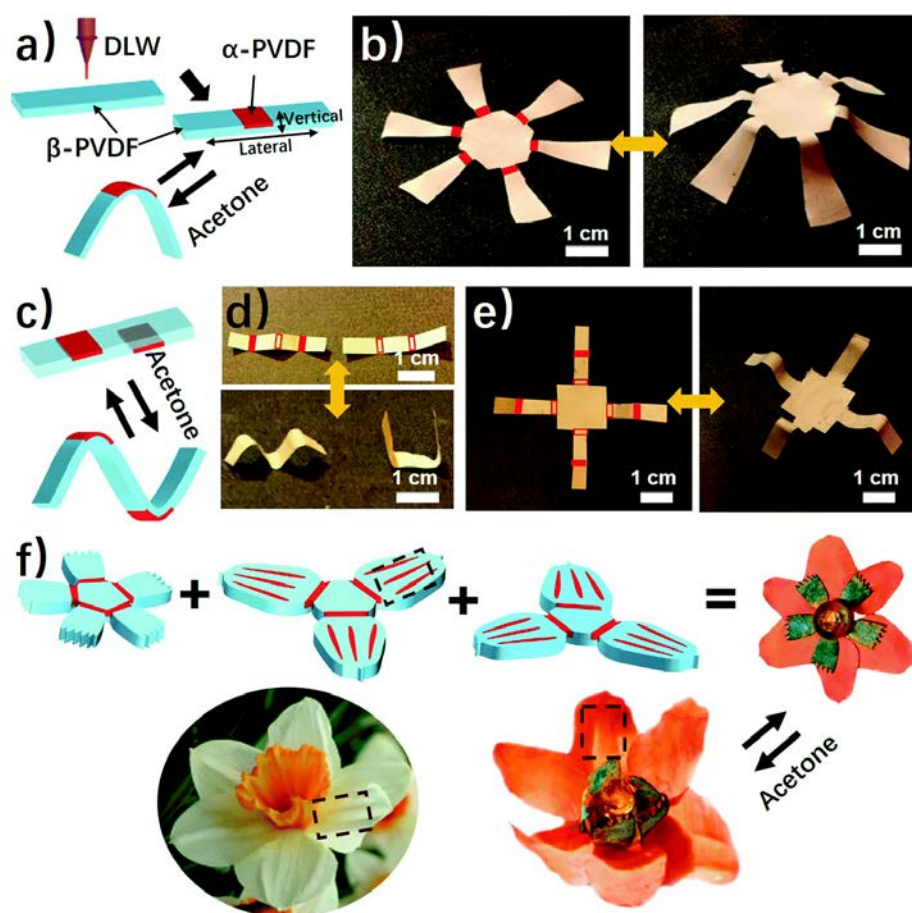
Figure 17. (**a**) Scheme of using direct laser writing to pattern the α phase domains in β phase PVDF film. (**b**) A photograph of the 3D structure transformed from a laser-patterned origami film. (**c**) A scheme of bidirectional folding of β phase PVDF film, resulting inform laser patterning on both sides. (**d**) A "MU" logo and (**e**) A 3D structure transformed from a to β phase PVDF film with laser patterning on both sides. (**f**) A PVDF blooming flower evolving from assembled multilayered PVDF films with each layer having origami patterns consisting of α and β phase origami patterns [209].

6. Conclusions and Perspective

The PVDF is one of the most challenging and interesting materials for the development of advanced applications due to its high dielectric constant, piezo-, pyro- and ferroelectric effects. Recent advances have been presented for β phase PVDF with the recent application possibilities in areas such as magnetoelectric materials, sensors, filtration membranes and biomedical applications. Despite significant progress has been made, some critically technical points are still needed for consideration for further applications. In general, they mainly include the following items: (i) The effective modification of homogeneous surface of PVDF films. A large roughness is harmful for electron transfer in electronic devices, which leads to a leak of current and reduce the device lifetime. (ii) The coupling mechanism for PVDF/electrodes interface should be further studied because the ferroelectric nature of PVDF likely induces the new barriers by gathering electron charge. This is important for the development of organic spin devices operated at room temperature. (iii) Seeking new techniques to enhance the efficiency for PVDF applications in Energy harvesting, tissue engineering, etc. This would be key step for the actual applications of PVDF devices. (iv) In addition, the geometries of PVDF with different crystal phases are needed to be studied in detail. This is very useful to get an insight on the relations between the morphology and the physical properties.

References

1. Lovinger, A.J. Poly(vinylidene fluoride). In *Developments in Crystalline Polymers—1*; Springer: Dordrecht, The Netherlands, 1982; pp. 195–273.

2. Lovinger, A.J. Annealing of poly(vinylidene fluoride) and formation of a fifth phase. *Macromolecules* **1982**, *15*, 40–44. [CrossRef]

3. Prest, W., Jr.; Luca, D. The formation of the γ phase from the α and β polymorphs of polyvinylidene fluoride. *J. Appl. Phys.* **1978**, *49*, 5042–5047. [CrossRef]

4. El Mohajir, B.-E.; Heymans, N. Changes in structural and mechanical behaviour of PVDF with processing and thermomechanical treatments. 1. Change in structure. *Polymer* **2001**, *42*, 5661–5667. [CrossRef]

5. Gregorio, R., Jr.; Cestari, M. Effect of crystallization temperature on the crystalline phase content and morphology of poly(vinylidene fluoride). *J. Polym. Sci. Part B Polym. Phys.* **1994**, *32*, 859–870. [CrossRef]

6. Salimi, A.; Yousefi, A. Analysis method: FTIR studies of β phase crystal formation in stretched PVDF films. *Polym. Test.* **2003**, *22*, 699–704. [CrossRef]

7. Pan, H.; Na, B.; Lv, R.; Li, C.; Zhu, J.; Yu, Z. Polar phase formation in poly(vinylidene fluoride) induced by melt annealing. *J. Polym. Sci. Part B Polym. Phys.* **2012**, *50*, 1433–1437. [CrossRef]

8. Kang, S.J.; Park, Y.J.; Sung, J.; Jo, P.S.; Park, C.; Kim, K.J.; Cho, B.O. Spin cast ferroelectric beta poly(vinylidene fluoride) thin films via rapid thermal annealing. *Appl. Phys. Lett.* **2008**, *92*, 012921. [CrossRef]

9. Song, R.; Yang, D.; He, L. Effect of surface modification of nanosilica on crystallization, thermal and mechanical properties of poly(vinylidene fluoride). *J. Mater. Sci.* **2007**, *42*, 8408–8417. [CrossRef]

10. Dutta, B.; Kar, E.; Bose, N.; Mukherjee, S. Significant enhancement of the electroactive β phase of PVDF by incorporating hydrothermally synthesized copper oxide nanoparticles. *RSC Adv.* **2015**, *5*, 105422–105434. [CrossRef]

11. Rutledge, G.; Carbeck, J.; Lacks, D. *Modeling the Electrical Properties of Polymers*; Technical Papers of the Annual Technical Conference-Society of Plastics Engineers Incorporated; Society Of Plastics Engineers Inc.: Indianapolis, IN, USA, 1996; pp. 2163–2166.

12. Lando, J.; Olf, H.; Peterlin, A. Nuclear magnetic resonance and X-ray determination of the structure of poly(vinylidene fluoride). *J. Polym. Sci. Part A Polym. Chem.* **1966**, *4*, 941–951. [CrossRef]

13. Wan, C.; Bowen, C.R. Multiscale-structuring of polyvinylidene fluoride for energy harvesting: The impact of molecular-, micro- and macro-structure. *J. Mater. Chem. A* **2017**, *5*, 3091–3128. [CrossRef]

14. Gregorio, R. Determination of the α, β, and γ crystalline phases of poly(vinylidene fluoride) films prepared at different conditions. *J. Appl. Polym. Sci.* **2006**, *100*, 3272–3279. [CrossRef]

15. Lopes, A.; Costa, C.M.; Tavares, C.; Neves, I.; Lanceros-Mendez, S. Nucleation of the electroactive γ phase and enhancement of the optical transparency in low filler content poly(vinylidene)/clay nanocomposites. *J. Phys. Chem. C* **2011**, *115*, 18076–18082. [CrossRef]

16. Martins, P.; Lopes, A.; Lanceros-Mendez, S. Electroactive phases of poly(vinylidene fluoride): Determination, processing and applications. *Prog. Polym. Sci.* **2014**, *39*, 683–706. [CrossRef]

17. Sajkiewicz, P.; Wasiak, A.; Gocłowski, Z. Phase transitions during stretching of poly(vinylidene fluoride). *Eur. Polym. J.* **1999**, *35*, 423–429. [CrossRef]

18. Bachmann, M.; Gordon, W.; Koenig, J.; Lando, J. An infrared study of phase-III poly(vinylidene fluoride). *J. Appl. Phys.* **1979**, *50*, 6106–6112. [CrossRef]

19. Boccaccio, T.; Bottino, A.; Capannelli, G.; Piaggio, P. Characterization of PVDF membranes by vibrational spectroscopy. *J. Membr. Sci.* **2002**, *210*, 315–329. [CrossRef]

20. Imamura, R.; Silva, A.; Gregorio, R. γ→β Phase transformation induced in poly(vinylidene fluoride) by stretching. *J. Appl. Polym. Sci.* **2008**, *110*, 3242–3246. [CrossRef]

21. Sim, L.; Majid, S.; Arof, A. Characteristics of PEMA/PVdF-HFP blend polymeric gel films incorporated with lithium triflate salt in electrochromic device. *Solid State Ion.* **2012**, *209*, 15–23. [CrossRef]

22. Sim, L.; Majid, S.; Arof, A. FTIR studies of PEMA/PVdF-HFP blend polymer electrolyte system incorporated with $LiCF_3SO_3$ salt. *Vib. Spectrosc.* **2012**, *58*, 57–66. [CrossRef]

23. Nalwa, H.S. *Ferroelectric Polymers: Chemistry: Physics, and Applications*; CRC Press: Boca Raton, FL, USA, 1995.

24. Lovinger, A.J. Crystallization of the β phase of poly(vinylidene fluoride) from the melt. *Polymer* **1981**, *22*, 412–413. [CrossRef]

25. Doll, W.; Lando, J. The polymorphism of poly(vinylidene fluoride) IV. The structure of high-pressure-crystallized poly(vinylidene fluoride). *J. Macromol. Sci. Part B* **1970**, *4*, 889–896. [CrossRef]

26. Yang, D.; Chen, Y. β phase formation of poly(vinylidene fluoride) from the melt induced by quenching. *J. Mater. Sci. Lett.* **1987**, *6*, 599–603. [CrossRef]

27. Broadhurst, M.; Davis, G.; McKinney, J.; Collins, R. Piezoelectricity and pyroelectricity in polyvinylidene fluoride—A model. *J. Appl. Phys.* **1978**, *49*, 4992–4997. [CrossRef]

28. Jungnickel, B. Poly(vinylidene fluoride) (overview). In *Polymeric Material Handbook*; Salamone, J.C., Ed.; CRC Press: New York, NY, USA, 1999.

29. Gregorio, R.; Ueno, E. Effect of crystalline phase, orientation and temperature on the dielectric properties of poly(vinylidene fluoride) (PVDF). *J. Mater. Sci.* **1999**, *34*, 4489–4500. [CrossRef]

30. Lanceros-Mendez, S.; Mano, J.; Costa, A.; Schmidt, V. FTIR and DSC studies of mechanically deformed β PVDF films. *J. Macromol. Sci. Part B* **2001**, *40*, 517–527. [CrossRef]

31. Luongo, J. Far-infrared spectra of piezoelectric polyvinylidene fluoride. *J. Polym. Sci. Part B Polym. Phys.* **1972**, *10*, 1119–1123. [CrossRef]

32. Kawai, H. The piezoelectricity of poly(vinylidene fluoride). *Jpn. J. Appl. Phys.* **1969**, *8*, 975. [CrossRef]

33. Li, L.; Zhang, M.; Rong, M.; Ruan, W. Studies on the transformation process of PVDF from α to β phase by stretching. *RSC Adv.* **2014**, *4*, 3938–3943. [CrossRef]

34. Sencadas, V.; Moreira, M.V.; Lanceros-Méndez, S.; Pouzada, A.S.; Filho, R.G. α to β Transformation on PVDF films obtained by uniaxial stretch. *Mater. Sci. Forum* **2006**, *514–516*, 872–876. [CrossRef]

35. Mohammadi, B.; Yousefi, A.A.; Bellah, S.M. Effect of tensile strain rate and elongation on crystalline structure and piezoelectric properties of PVDF thin films. *Polym. Test.* **2007**, *26*, 42–50. [CrossRef]

36. Hattori, T.; Kanaoka, M.; Ohigashi, H. Improved piezoelectricity in thick lamellar β form crystals of poly(vinylidene fluoride) crystallized under high pressure. *J. Appl. Phys.* **1996**, *79*, 2016–2022. [CrossRef]

37. Sharma, M.; Madras, G.; Bose, S. Process induced electroactive β polymorph in PVDF: Effect on dielectric and ferroelectric properties. *Phys. Chem. Chem. Phys.* **2014**, *16*, 14792–14799. [CrossRef] [PubMed]

38. Bohlen, M.; Bolton, K. Inducing the β phase of poly(vinylidene fluoride)—A review. *Annu. Rev. Nanosci. Nanotechnol.* **2014**, *1*, 150110.

39. Ramos, M.M.; Correia, H.M.; Lanceros-Mendez, S. Atomistic modelling of processes involved in poling of PVDF. *Comput. Mater. Sci.* **2005**, *33*, 230–236. [CrossRef]

40. Schwartz, M. *Encyclopedia of Smart Materials*; Wiley: New York, NY, USA, 2002; p. 811.

41. Hsu, S.; Lu, F.; Waldman, D.; Muthukumar, M. Analysis of the crystalline phase transformation of poly(vinylidene fluoride). *Macromolecules* **1985**, *18*, 2583–2587. [CrossRef]

42. Southgate, P. Room-temperature poling and morphology changes in pyroelectric polyvinylidene fluoride. *Appl. Phys. Lett.* **1976**, *28*, 250–252. [CrossRef]

43. Martín, J.; Zhao, D.; Lenz, T.; Katsouras, I.; de Leeuw, D.M.; Stingelin, N. Solid-state-processing of δ PVDF. *Mater. Horiz.* **2017**, *4*, 408–414. [CrossRef]

44. Rastogi, A.C.; Desu, S.B. Ferroelectric Poly(vinylidene fluoride) Thin Films Grown by Low-Pressure Chemical Vapor Polymerization. *Chem. Vap. Depos.* **2006**, *12*, 742–750. [CrossRef]

45. Benz, M.; Euler, W.B.; Gregory, O.J. The role of solution phase water on the deposition of thin films of poly(vinylidene fluoride). *Macromolecules* **2002**, *35*, 2682–2688. [CrossRef]

46. Ribeiro, C.; Sencadas, V.; Ribelles, J.L.G.; Lanceros-Méndez, S. Influence of processing conditions on polymorphism and nanofiber morphology of electroactive poly(vinylidene fluoride) electrospun membranes. *Soft Mater.* **2010**, *8*, 274–287. [CrossRef]

47. Ramakrishna, S.; Fujihara, K.; Teo, W.; Lim, T.-C.; Ma, Z. *An Introduction to Electrospinning and Nanofibers*; World Scientific Publishing Company: Singapore, 2005.

48. Andrew, J.; Mack, J.; Clarke, D. Electrospinning of polyvinylidene difluoride-based nanocomposite fibers. *J. Mater. Res.* **2008**, *23*, 105–114. [CrossRef]

49. Ren, X.; Dzenis, Y. Novel continuous poly(vinylidene fluoride) nanofibers. *MRS Online Proc. Libr. Arch.* **2006**, *920*. [CrossRef]

50. Zhao, Z.; Li, J.; Yuan, X.; Li, X.; Zhang, Y.; Sheng, J. Preparation and properties of electrospun poly(vinylidene fluoride) membranes. *J. Appl. Polym. Sci.* **2005**, *97*, 466–474. [CrossRef]

51. Zheng, J.; He, A.; Li, J.; Han, C.C. Polymorphism control of poly(vinylidene fluoride) through electrospinning. *Macromol. Rapid Commun.* **2007**, *28*, 2159–2162. [CrossRef]

52. Yee, W.A.; Kotaki, M.; Liu, Y.; Lu, X. Morphology, polymorphism behavior and molecular orientation of electrospun poly(vinylidene fluoride) fibers. *Polymer* **2007**, *48*, 512–521. [CrossRef]

53. Choi, S.W.; Jo, S.M.; Lee, W.S.; Kim, Y.R. An electrospun poly(vinylidene fluoride) nanofibrous membrane and its battery applications. *Adv. Mater.* **2003**, *15*, 2027–2032. [CrossRef]

54. Xiao, Q.; Wang, X.; Li, W.; Li, Z.; Zhang, T.; Zhang, H. Macroporous polymer electrolytes based on PVDF/PEO-*b*-PMMA block copolymer blends for rechargeable lithium ion battery. *J. Membr. Sci.* **2009**, *334*, 117–122. [CrossRef]

55. Klinge, U.; Klosterhalfen, B.; Öttinger, A.; Junge, K.; Schumpelick, V. PVDF as a new polymer for the construction of surgical meshes. *Biomaterials* **2002**, *23*, 3487–3493. [CrossRef]

56. Choi, S.W.; Kim, J.R.; Ahn, Y.R.; Jo, S.M.; Cairns, E.J. Characterization of electrospun PVDF fiber-based polymer electrolytes. *Chem. Mater.* **2007**, *19*, 104–115. [CrossRef]

57. Roberts, G. *Langmuir–Blodgett Films*; Springer Science & Business Media: Berlin, Germany, 2013.

58. Chen, S.; Li, X.; Yao, K.; Tay, F.E.H.; Kumar, A.; Zeng, K. Self-polarized ferroelectric PVDF homopolymer ultra-thin films derived from Langmuir–Blodgett deposition. *Polymer* **2012**, *53*, 1404–1408. [CrossRef]

59. Jiang, Y.; Ye, Y.; Yu, J.; Yang, Y.; Xu, J.; Wu, Z. A study on ferroelectric PVDF ultrathin films prepared by LB technique. *Integr. Ferroelectr.* **2007**, *88*, 21–26. [CrossRef]

60. Jones, C.A.; Petty, M.C.; Roberts, G.G. Langmuir–Blodgett films: A new class of pyroelectric materials. *IEEE Trans. Ultrason. Ferroelectr. Freq. Control* **1988**, *35*, 736–740. [CrossRef] [PubMed]

61. Zhu, H.; Mitsuishi, M.; Miyashita, T. Facile Preparation of Highly Oriented Poly(vinylidene fluoride) Langmuir–Blodgett Nanofilms Assisted by Amphiphilic Polymer Nanosheets. *Macromolecules* **2012**, *45*, 9076–9084. [CrossRef]

62. Zhu, H.; Yamamoto, S.; Matsui, J.; Miyashita, T.; Mitsuishi, M. Asymmetric Ferroelectric Switching Based on an Al/PVDF Langmuir–Blodgett Nanofilm/PEDOT:PSS/Al Device. *Mol. Cryst. Liq. Cryst.* **2015**, *618*, 89–94. [CrossRef]

63. Kliem, H.; Tadros-Morgane, R. Extrinsic versus intrinsic ferroelectric switching: Experimental investigations using ultra-thin PVDF Langmuir–Blodgett films. *J. Phys. D Appl. Phys.* **2005**, *38*, 1860. [CrossRef]

64. Zhang, X.; Tong, J.; Zhu, H.; Wang, Z.; Zhou, L.; Wang, S.; Miyashita, T.; Mitsuishi, M.; Qin, G. Room temperature magnetoresistance effects in ferroelectric poly(vinylidene fluoride) spin valves. *J. Mater. Chem. C* **2017**, *5*, 5055–5062. [CrossRef]

65. Ramasundaram, S.; Yoon, S.; Kim, K.J.; Lee, J.S. Direct Preparation of Nanoscale Thin Films of Poly(vinylidene fluoride) Containing β Crystalline Phase by Heat-Controlled Spin Coating. *Macromol. Chem. Phys.* **2008**, *209*, 2516–2526. [CrossRef]

66. Ramasundaram, S.; Yoon, S.; Kim, K.J.; Lee, J.S.; Park, C. Crystalline structure and ferroelectric response of poly(vinylidene fluoride)/organically modified silicate thin films prepared by heat controlled spin coating. *Macromol. Chem. Phys.* **2009**, *210*, 951–960. [CrossRef]

67. Cardoso, V.; Minas, G.; Costa, C.M.; Tavares, C.; Lanceros-Mendez, S. Micro and nanofilms of poly(vinylidene fluoride) with controlled thickness, morphology and electroactive crystalline phase for sensor and actuator applications. *Smart Mater. Struct.* **2011**, *20*, 087002. [CrossRef]

68. He, X.; Yao, K. Crystallization mechanism and piezoelectric properties of solution-derived ferroelectric poly(vinylidene fluoride) thin films. *Appl. Phys. Lett.* **2006**, *89*, 112909. [CrossRef]

69. Sakata, J.; Mochizuki, M. Preparation of organic thin films by an electrospray technique I. Crystal forms and their orientation in poly(vinylidene flouride) films. *Thin Solid Films* **1991**, *195*, 175–184. [CrossRef]

70. Park, S.H.; Lee, D.C. A study of the electrical stability characteristics of a PVDF organic thin film fabricated by using the thermal vapor deposition method. *J. Korean Phys. Soc.* **1999**, *35*, 431–437.

71. Noda, K.; Ishida, K.; Horiuchi, T.; Matsushige, K.; Kubono, A. Structures of vinylidene fluoride oligomer thin films on alkali halide substrate. *J. Appl. Phys.* **1999**, *86*, 3688–3693. [CrossRef]

72. Ouyang, J.; Chu, C.-W.; Tseng, R.J.-H.; Prakash, A.; Yang, Y. Organic memory device fabricated through solution processing. *Proc. IEEE* **2005**, *93*, 1287–1296. [CrossRef]

73. Mcculloch, I. Thin films: Rolling out organic electronics. *Nat. Mater.* **2005**, *4*, 583–584. [CrossRef] [PubMed]

74. Sencadas, V.; Filho, R.G.; Lanceros-Mendez, S. Processing and characterization of a novel nonporous poly(vinilidene fluoride) films in the β phase. *J. Non-Cryst. Solids* **2006**, *352*, 2226–2229. [CrossRef]

75. Branciforti, M.C.; Sencadas, V.; Lanceros-Mendez, S.; Gregorio, R. New technique of processing highly oriented poly(vinylidene fluoride) films exclusively in the β phase. *J. Polym. Sci. Part B Polym. Phys.* **2007**, *45*, 2793–2801. [CrossRef]

76. Voet, V.S.D.; Hermida-Merino, D.; ten Brinke, G.; Loos, K. Block copolymer route towards poly(vinylidene fluoride)/poly(methacrylic acid)/nickel nanocomposites. *RSC Adv.* **2013**, *3*, 7938–7946. [CrossRef]

77. Golzari, N.; Adams, J.; Beuermann, S. Inducing β phase crystallinity in block copolymers of vinylidene fluoride with methyl methacrylate or styrene. *Polymers* **2017**, *9*, 306. [CrossRef]

78. Lovinger, A.J.; Furukawa, T.; Davis, G.; Broadhurst, M. Crystallographic changes characterizing the Curie transition in three ferroelectric copolymers of vinylidene fluoride and trifluoroethylene: 1. As-crystallized samples. *Polymer* **1983**, *24*, 1225–1232. [CrossRef]

79. Furukawa, T.; Johnson, G.; Bair, H.; Tajitsu, Y.; Chiba, A.; Fukada, E. Ferroelectric phase transition in a copolymer of vinylidene fluoride and trifluoroethylene. *Ferroelectrics* **1981**, *32*, 61–67. [CrossRef]

80. Ohigashi, H.; Omote, K.; Gomyo, T. Formation of "single crystalline films" of ferroelectric copolymers of vinylidene fluoride and trifluoroethylene. *Appl. Phys. Lett.* **1995**, *66*, 3281–3283. [CrossRef]

81. Künstler, W.; Wegener, M.; Seiß, M.; Gerhard-Multhaupt, R. Preparation and assessment of piezo- and pyroelectric poly(vinylidene fluoride-hexafluoropropylene) copolymer films. *Appl. Phys. A Mater. Sci. Process.* **2001**, *73*, 641–645. [CrossRef]

82. Huan, Y.; Liu, Y.; Yang, Y. Simultaneous stretching and static electric field poling of poly(vinylidene fluoride-hexafluoropropylene) copolymer films. *Polym. Eng. Sci.* **2007**, *47*, 1630–1633. [CrossRef]

83. Ameduri, B. From vinylidene fluoride (VDF) to the applications of VDF-containing polymers and copolymers: Recent developments and future trends. *Chem. Rev.* **2009**, *109*, 6632–6686. [CrossRef] [PubMed]

84. Li, Z.; Wang, Y.; Cheng, Z.-Y. Electromechanical properties of poly(vinylidene-fluoride-chlorotrifluoroethylene) copolymer. *Appl. Phys. Lett.* **2006**, *88*, 062904. [CrossRef]

85. Ye, H.J.; Shao, W.Z.; Zhen, L. Crystallization kinetics and phase transformation of poly(vinylidene fluoride) films incorporated with functionalized baTiO$_3$ nanoparticles. *J. Appl. Polym. Sci.* **2013**, *129*, 2940–2949. [CrossRef]

86. Mendes, S.F.; Costa, C.M.; Caparrós, C.; Sencadas, V.; Lanceros-Méndez, S. Effect of filler size and concentration on the structure and properties of poly(vinylidene fluoride)/BaTiO$_3$ nanocomposites. *J. Mater. Sci.* **2012**, *47*, 1378–1388. [CrossRef]

87. Priya, L.; Jog, J. Poly(vinylidene fluoride)/clay nanocomposites prepared by melt intercalation: Crystallization and dynamic mechanical behavior studies. *J. Polym. Sci. Part B Polym. Phys.* **2002**, *40*, 1682–1689. [CrossRef]

88. Ma, W.; Zhang, J.; Chen, S.; Wang, X. β Phase of poly(vinylidene fluoride) formation in poly(vinylidene fluoride)/poly(methyl methacrylate) blend from solutions. *Appl. Surf. Sci.* **2008**, *254*, 5635–5642. [CrossRef]

89. An, N.; Liu, H.; Ding, Y.; Zhang, M.; Tang, Y. Preparation and electroactive properties of a PVDF/nano-TiO$_2$ composite film. *Appl. Surf. Sci.* **2011**, *257*, 3831–3835. [CrossRef]

90. Martins, P.; Caparros, C.; Gonçalves, R.; Martins, P.; Benelmekki, M.; Botelho, G.; Lanceros-Mendez, S. Role of nanoparticle surface charge on the nucleation of the electroactive β poly(vinylidene fluoride) nanocomposites for sensor and actuator applications. *J. Phys. Chem. C* **2012**, *116*, 15790–15794. [CrossRef]

91. Wang, W.; Zhang, S.; Srisombat, L.-O.; Lee, T.R.; Advincula, R.C. Gold-Nanoparticle- and Gold-Nanoshell-Induced Polymorphism in Poly(vinylidene fluoride). *Macromol. Mater. Eng.* **2011**, *296*, 178–184. [CrossRef]

92. Xing, C.; Zhao, L.; You, J.; Dong, W.; Cao, X.; Li, Y. Impact of ionic liquid-modified multiwalled carbon nanotubes on the crystallization behavior of poly(vinylidene fluoride). *J. Phys. Chem. B* **2012**, *116*, 8312–8320. [CrossRef] [PubMed]

93. Xing, C.; Guan, J.; Li, Y.; Li, J. Effect of a room-temperature ionic liquid on the structure and properties of electrospun poly(vinylidene fluoride) nanofibers. *ACS Appl. Mater. Interfaces* **2014**, *6*, 4447–4457. [CrossRef] [PubMed]

94. Martins, P.; Costa, C.M.; Lanceros-Mendez, S. Nucleation of electroactive β phase poly(vinilidene fluoride) with CoFe$_2$O$_4$ and NiFe$_2$O$_4$ nanofillers: A new method for the preparation of multiferroic nanocomposites. *Appl. Phys. A* **2011**, *103*, 233–237. [CrossRef]

95. Martins, P.; Costa, C.M.; Benelmekki, M.; Botelho, G.; Lanceros-Mendez, S. On the origin of the electroactive poly(vinylidene fluoride) β phase nucleation by ferrite nanoparticles via surface electrostatic interactions. *CrystEngComm* **2012**, *14*, 2807–2811. [CrossRef]

96. Bergman, J.G., Jr.; McFee, J.H.; Crane, G.R. Pyroelectricity and optical second harmonic generation in polyvinylidene fluoride films. *Appl. Phys. Lett.* **1971**, *18*, 203–205. [CrossRef]

97. Nakamura, K.I.; Wada, Y. Piezoelectricity, pyroelectricity, and the electrostriction constant of poly(vinylidene fluoride). *J. Polym. Sci. Part B Polym. Phys.* **1971**, *9*, 161–173. [CrossRef]

98. Fukada, E. History and recent progress in piezoelectric polymers. *IEEE Trans. Ultrason. Ferroelectr. Freq. Control* **2000**, *47*, 1277–1290. [CrossRef] [PubMed]

99. Bune, A.; Zhu, C.; Ducharme, S.; Blinov, L.; Fridkin, V.; Palto, S.; Petukhova, N.; Yudin, S. Piezoelectric and pyroelectric properties of ferroelectric Langmuir–Blodgett polymer films. *J. Appl. Phys.* **1999**, *85*, 7869–7873. [CrossRef]

100. Gomes, J.; Nunes, J.S.; Sencadas, V.; Lanceros-Méndez, S. Influence of the β phase content and degree of crystallinity on the piezo- and ferroelectric properties of poly(vinylidene fluoride). *Smart Mater. Struct.* **2010**, *19*, 065010. [CrossRef]

101. Dargaville, T.R.; Celina, M.; Chaplya, P.M. Evaluation of piezoelectric poly(vinylidene fluoride) polymers for use in space environments. I. Temperature limitations. *J. Polym. Sci. Part B Polym. Phys.* **2005**, *43*, 1310–1320. [CrossRef]

102. Nix, E.; Ward, I. The measurement of the shear piezoelectric coefficients of polyvinylidene fluoride. *Ferroelectrics* **1986**, *67*, 137–141. [CrossRef]

103. Lang, S.B.; Das-Gupta, D.K. Pyroelectricity: Fundamentals and applications. In *Handbook of Advanced Electronic and Photonic Materials and Devices*; Elsevier: Amsterdam, The Netherlands, 2001; pp. 1–55.

104. Kepler, R.; Anderson, R. Piezoelectricity and pyroelectricity in polyvinylidene fluoride. *J. Appl. Phys.* **1978**, *49*, 4490–4494. [CrossRef]

105. Chynoweth, A. Dynamic method for measuring the pyroelectric effect with special reference to barium titanate. *J. Appl. Phys.* **1956**, *27*, 78–84. [CrossRef]

106. Roberts, G. Polar Langmuir–Blodgett thin film layers for non-linear optical and pyroelectric applications. *Ferroelectrics* **1989**, *91*, 21–38. [CrossRef]

107. Lines, M.E.; Glass, A.M. *Principles and Applications of Ferroelectrics and Related Materials*; Oxford University Press: Oxford, UK, 1977.

108. Sagar, R.; Gaur, S.S.; Gaur, M. Effect of $BaZrO_3$ nanoparticles on pyroelectric properties of polyvinylidene fluoride (PVDF). *J. Therm. Anal. Calorim.* **2017**, *128*, 1235–1239. [CrossRef]

109. Furukawa, T.; Date, M.; Fukada, E. Hysteresis phenomena in polyvinylidene fluoride under high electric field. *J. Appl. Phys.* **1980**, *51*, 1135–1141. [CrossRef]

110. Zhu, H.; Yamamoto, S.; Matsui, J.; Miyashita, T.; Mitsuishi, M. Ferroelectricity of poly(vinylidene fluoride) homopolymer Langmuir–Blodgett nanofilms. *J. Mater. Chem. C* **2014**, *2*, 6727–6731. [CrossRef]

111. Furukawa, T. Ferroelectric properties of vinylidene fluoride copolymers. *Phase Transit. A Multinatl. J.* **1989**, *18*, 143–211. [CrossRef]

112. Kepler, R.G.; Anderson, R. Ferroelectric polymers. *Adv. Phys.* **1992**, *41*, 1–57. [CrossRef]

113. Naber, R.C.; Asadi, K.; Blom, P.W.; de Leeuw, D.M.; de Boer, B. Organic nonvolatile memory devices based on ferroelectricity. *Adv. Mater.* **2010**, *22*, 933–945. [CrossRef] [PubMed]

114. Choi, S.-S.; Lee, Y.S.; Joo, C.W.; Lee, S.G.; Park, J.K.; Han, K.-S. Electrospun PVDF nanofiber web as polymer electrolyte or separator. *Electrochim. Acta* **2004**, *50*, 339–343. [CrossRef]

115. Abbrent, S.; Plestil, J.; Hlavata, D.; Lindgren, J.; Tegenfeldt, J.; Wendsjö, Å. Crystallinity and morphology of PVdF–HFP-based gel electrolytes. *Polymer* **2001**, *42*, 1407–1416. [CrossRef]

116. Tsuchida, E.; Ohno, H.; Tsunemi, K. Conduction of lithium ions in polyvinylidene fluoride and its derivatives—I. *Electrochim. Acta* **1983**, *28*, 591–595. [CrossRef]

117. Voice, A.; Southall, J.; Rogers, V.; Matthews, K.; Davies, G.; McIntyre, J.; Ward, I. Thermoreversible polymer gel electrolytes. *Polymer* **1994**, *35*, 3363–3372. [CrossRef]

118. Elimelech, M.; Phillip, W.A. The future of seawater desalination: Energy, technology, and the environment. *Science* **2011**, *333*, 712–717. [CrossRef] [PubMed]

119. Jiang, X.C.; Ding, J.; Kumar, A. Polyurethane–poly(vinylidene fluoride) (PU–PVDF) thin film composite membranes for gas separation. *J. Membr. Sci.* **2008**, *323*, 371–378. [CrossRef]

120. Razmjou, A.; Arifin, E.; Dong, G.; Mansouri, J.; Chen, V. Superhydrophobic modification of TiO$_2$ nanocomposite PVDF membranes for applications in membrane distillation. *J. Membr. Sci.* **2012**, *415*, 850–863. [CrossRef]

121. Peng, P.; Shi, B.; Lan, Y. A review of membrane materials for ethanol recovery by pervaporation. *Sep. Sci. Technol.* **2010**, *46*, 234–246. [CrossRef]

122. Song, H.; Shao, J.; Wang, J.; Zhong, X. The removal of natural organic matter with LiCl–TiO$_2$-doped PVDF membranes by integration of ultrafiltration with photocatalysis. *Desalination* **2014**, *344*, 412–421. [CrossRef]

123. Ambashta, R.D.; Sillanpää, M.E. Membrane purification in radioactive waste management: A short review. *J. Environ. Radioact.* **2012**, *105*, 76–84. [CrossRef] [PubMed]

124. Zaviska, F.; Drogui, P.; Grasmick, A.; Azais, A.; Héran, M. Nanofiltration membrane bioreactor for removing pharmaceutical compounds. *J. Membr. Sci.* **2013**, *429*, 121–129. [CrossRef]

125. Li, M.; Katsouras, I.; Piliego, C.; Glasser, G.; Lieberwirth, I.; Blom, P.W.; de Leeuw, D.M. Controlling the microstructure of poly(vinylidene-fluoride) (PVDF) thin films for microelectronics. *J. Mater. Chem. C* **2013**, *1*, 7695–7702. [CrossRef]

126. Zhou, B.; Powell, A.C. Phase field simulations of early stage structure formation during immersion precipitation of polymeric membranes in 2D and 3D. *J. Membr. Sci.* **2006**, *268*, 150–164. [CrossRef]

127. Benz, M.; Rosenberg, K.J.; Kramer, E.J.; Israelachvili, J.N. The deformation and adhesion of randomly rough and patterned surfaces. *J. Phys. Chem. B* **2006**, *110*, 11884–11893. [CrossRef] [PubMed]

128. Tamura, M.; Yamaguchi, T.; Oyaba, T.; Yoshimi, T. Electroacoustic transducers with piezoelectric high polymer films. *J. Audio Eng. Soc.* **1975**, *23*, 21–26.

129. Ribeiro, C.; Panadero, J.; Sencadas, V.; Lanceros-Méndez, S.; Tamano, M.; Moratal, D.; Salmerón-Sánchez, M.; Ribelles, J.G. Fibronectin adsorption and cell response on electroactive poly(vinylidene fluoride) films. *Biomed. Mater.* **2012**, *7*, 035004. [CrossRef] [PubMed]

130. Jeon, J.-H.; Kang, S.-P.; Lee, S.; Oh, I.-K. Novel biomimetic actuator based on SPEEK and PVDF. *Sens. Actuators B Chem.* **2009**, *143*, 357–364. [CrossRef]

131. Panwar, V.; Cha, K.; Park, J.-O.; Park, S. High actuation response of PVDF/PVP/PSSA based ionic polymer metal composites actuator. *Sens. Actuators B Chem.* **2012**, *161*, 460–470. [CrossRef]

132. Zhang, Y.; Niu, H.; Xie, S.; Zhang, X. Numerical and experimental investigation of active vibration control in a cylindrical shell partially covered by a laminated PVDF actuator. *Smart Mater. Struct.* **2008**, *17*, 035024. [CrossRef]

133. Chen, Z.; Kwon, K.-Y.; Tan, X. Integrated IPMC/PVDF sensory actuator and its validation in feedback control. *Sens. Actuators A Phys.* **2008**, *144*, 231–241. [CrossRef]

134. Snyder, S.D.; Tanaka, N.; Kikushima, Y. The use of optimally shaped piezo-electric film sensors in the active control of free field structural radiation, Part 2: Feedback control. *J. Vib. Acoust.* **1996**, *118*, 112–121. [CrossRef]

135. Shirinov, A.; Schomburg, W. Pressure sensor from a PVDF film. *Sens. Actuators A Phys.* **2008**, *142*, 48–55. [CrossRef]

136. Fujitsuka, N.; Sakata, J.; Miyachi, Y.; Mizuno, K.; Ohtsuka, K.; Taga, Y.; Tabata, O. Monolithic pyroelectric infrared image sensor using PVDF thin film. *Sens. Actuators A Phys.* **1998**, *66*, 237–243. [CrossRef]

137. Murayama, N.; Nakamura, K.; Obara, H.; Segawa, M. The strong piezoelectricity in polyvinylidene fluroide (PVDF). *Ultrasonics* **1976**, *14*, 15–24. [CrossRef]

138. Hurmila, S.; Stubb, H.; Pitkänen, J.; Lahdenperä, K.; Penttinen, A.; Suorsa, V.; Tauriainen, A. Ultrasonic transducers using PVDF. *Ferroelectrics* **1991**, *115*, 267–278. [CrossRef]

139. Mazurek, B.; Janiczek, T.; Chmielowiec, J. Assessment of vehicle weight measurement method using PVDF transducers. *J. Electrost.* **2001**, *51*, 76–81. [CrossRef]

140. Xu, G.; Zhang, M.; Zhou, Q.; Chen, H.; Gao, T.; Li, C.; Shi, G. A small graphene oxide sheet/polyvinylidene fluoride bilayer actuator with large and rapid responses to multiple stimuli. *Nanoscale* **2017**, *9*, 17465–17470. [CrossRef] [PubMed]

141. Wang, F.; Ko, S.Y.; Park, J.O.; Park, S.H.; Kee, C.D. Electroactive polymer actuator based on PVDF and graphene through electrospinning. *Adv. Mater. Res.* **2015**, *1105*, 311–314. [CrossRef]

142. Fukushima, T.; Asaka, K.; Kosaka, A.; Aida, T. Fully Plastic Actuator through Layer-by-Layer Casting with Ionic-Liquid-Based Bucky Gel. *Angew. Chem. Int. Ed.* **2005**, *44*, 2410–2413. [CrossRef] [PubMed]

143. Mukai, K.; Asaka, K.; Kiyohara, K.; Sugino, T.; Takeuchi, I.; Fukushima, T.; Aida, T. High performance fully plastic actuator based on ionic-liquid-based bucky gel. *Electrochim. Acta* **2008**, *53*, 5555–5562. [CrossRef]

144. Saketi, P.; Latifi, S.K.; Hirvonen, J.; Rajala, S.; Vehkaoja, A.; Salpavaara, T.; Lekkala, J.; Kallio, P. PVDF microforce sensor for the measurement of Z-directional strength in paper fiber bonds. *Sens. Actuators A Phys.* **2015**, *222*, 194–203. [CrossRef]

145. Choi, S.-C.; Park, J.-S.; Kim, J.-H. Active damping of rotating composite thin-walled beams using MFC actuators and PVDF sensors. *Compos. Struct.* **2006**, *76*, 362–374. [CrossRef]

146. Ying, Z.; Jiang, Y.; Du, X.; Xie, G.; Yu, J.; Wang, H. PVDF coated quartz crystal microbalance sensor for DMMP vapor detection. *Sens. Actuators B Chem.* **2007**, *125*, 167–172. [CrossRef]

147. Shin, K.-Y.; Lee, J.S.; Jang, J. Highly sensitive, wearable and wireless pressure sensor using free-standing ZnO nanoneedle/PVDF hybrid thin film for heart rate monitoring. *Nano Energy* **2016**, *22*, 95–104. [CrossRef]

148. Yoon, S.; Prabu, A.A.; Ramasundaram, S.; Kim, K.J. PVDF nanoweb touch sensors prepared using electro-spinning process for smart apparels applications. *Adv. Sci. Technol.* **2008**, *60*, 52–57. [CrossRef]

149. Wang, Y.; Zheng, J.; Ren, G.; Zhang, P.; Xu, C. A flexible piezoelectric force sensor based on PVDF fabrics. *Smart Mater. Struct.* **2011**, *20*, 045009. [CrossRef]

150. Al-Saygh, A.; Ponnamma, D.; AlMaadeed, M.A.; Poornima Vijayan, P.; Karim, A.; Hassan, M.K. Flexible Pressure Sensor Based on PVDF Nanocomposites Containing Reduced Graphene Oxide-Titania Hybrid Nanolayers. *Polymers* **2017**, *9*, 33. [CrossRef]

151. Martins, P.; Lasheras, A.; Gutierrez, J.; Barandiaran, J.; Orue, I.; Lanceros-Mendez, S. Optimizing piezoelectric and magnetoelectric responses on $CoFe_2O_4$/P(VDF-TrFE) nanocomposites. *J. Phys. D Appl. Phys.* **2011**, *44*, 495303. [CrossRef]

152. Spanu, A.; Pinna, L.; Viola, F.; Seminara, L.; Valle, M.; Bonfiglio, A.; Cosseddu, P. A high-sensitivity tactile sensor based on piezoelectric polymer PVDF coupled to an ultra-low voltage organic transistor. *Org. Electron.* **2016**, *36*, 57–60. [CrossRef]

153. Scott, J.C.; Bozano, L.D. Nonvolatile memory elements based on organic materials. *Adv. Mater.* **2007**, *19*, 1452–1463. [CrossRef]

154. Singh, T.B.; Marjanović, N.; Matt, G.; Sariciftci, N.; Schwödiauer, R.; Bauer, S. Nonvolatile organic field-effect transistor memory element with a polymeric gate electret. *Appl. Phys. Lett.* **2004**, *85*, 5409–5411. [CrossRef]

155. Li, Y.; Sinitskii, A.; Tour, J.M. Electronic two-terminal bistable graphitic memories. *Nat. Mater.* **2008**, *7*, 966–971. [CrossRef] [PubMed]

156. Liang, S.; Yang, H.; Yang, H.; Tao, B.; Djeffal, A.; Chshiev, M.; Huang, W.; Li, X.; Ferri, A.; Desfeux, R. Ferroelectric control of organic/ferromagnetic spinterface. *Adv. Mater.* **2016**, *28*, 10204–10210. [CrossRef] [PubMed]

157. Eerenstein, W.; Mathur, N.; Scott, J.F. Multiferroic and magnetoelectric materials. *Nature* **2006**, *442*, 759–765. [CrossRef] [PubMed]

158. Kleemann, W.; Binek, C. Multiferroic and magnetoelectric materials. In *Magnetic Nanostructures*; Springer: Berlin, Germany, 2013; pp. 163–187.

159. Martins, P.; Lanceros-Méndez, S. Polymer-based magnetoelectric materials. *Adv. Funct. Mater.* **2013**, *23*, 3371–3385. [CrossRef]

160. Dong, X.; Wang, B.; Wang, K.; Wan, J.; Liu, J.M. Ultra-sensitive detection of magnetic field and its direction using bilayer PVDF/Metglas laminate. *Sens. Actuators A Phys.* **2009**, *153*, 64–68. [CrossRef]

161. Qi, Y.; Jafferis, N.T.; Lyons, K., Jr.; Lee, C.M.; Ahmad, H.; McAlpine, M.C. Piezoelectric ribbons printed onto rubber for flexible energy conversion. *Nano Lett.* **2010**, *10*, 524–528. [CrossRef] [PubMed]

162. Gutiérrez, J.; Lasheras, A.; Barandiarán, J.M.; Vilas, J.L.; Sebastián, M.S.; León, L.M. Temperature response of magnetostrictive/piezoelectric polymer magnetoelectric laminates. *MRS Online Proc. Libr. Arch.* **2012**, *1398*. [CrossRef]

163. Fiebig, M. Revival of the magnetoelectric effect. *J. Phys. D Appl. Phys.* **2005**, *38*, R123. [CrossRef]

164. Nan, C.; Bichurin, M.; Dong, S.; Viehland, D.; Srinivasan, G. Multiferroic magnetoelectric composites: Historical perspective, status, and future directions. *J. Appl. Phys.* **2008**, *103*, 031101. [CrossRef]

165. Chu, Y.-H.; Martin, L.W.; Holcomb, M.B.; Gajek, M.; Han, S.-J.; He, Q.; Balke, N.; Yang, C.-H.; Lee, D.; Hu, W. Electric-field control of local ferromagnetism using a magnetoelectric multiferroic. *Nat. Mater.* **2008**, *7*, 478–482. [CrossRef] [PubMed]

166. Scott, J.; Morrison, F.; Miyake, M.; Zubko, P. Nano-ferroelectric materials and devices. *Ferroelectrics* **2006**, *336*, 237–245. [CrossRef]

167. Zhai, J.; Dong, S.; Xing, Z.; Li, J.; Viehland, D. Giant magnetoelectric effect in Metglas/polyvinylidene-fluoride laminates. *Appl. Phys. Lett.* **2006**, *89*, 083507. [CrossRef]

168. Yang, F.; Wen, Y.; Li, P.; Zheng, M. Magnetoelectric response of magnetostrictive/piezoelectric/magnetostrictive laminate composite. In Proceedings of the 2006 IEEE International Conference on Information Acquisition, Weihai, China, 20–23 August 2006; pp. 1010–1014.

169. Lasheras, A.; Gutiérrez, J.; Reis, S.; Sousa, D.; Silva, M.; Martins, P.; Lanceros-Mendez, S.; Barandiarán, J.; Shishkin, D.; Potapov, A. Energy harvesting device based on a metallic glass/PVDF magnetoelectric laminated composite. *Smart Mater. Struct.* **2015**, *24*, 065024. [CrossRef]

170. Fang, Z.; Lu, S.; Li, F.; Datta, S.; Zhang, Q.; El Tahchi, M. Enhancing the magnetoelectric response of Metglas/polyvinylidene fluoride laminates by exploiting the flux concentration effect. *Appl. Phys. Lett.* **2009**, *95*, 112903. [CrossRef]

171. Fetisov, L.; Baraban, I.; Fetisov, Y.K.; Burdin, D.; Vopson, M. Nonlinear magnetoelectric effects in flexible composite ferromagnetic—Piezopolymer structures. *J. Magn. Magn. Mater.* **2017**, *441*, 628–634. [CrossRef]

172. Mori, K.; Wuttig, M. Magnetoelectric coupling in Terfenol-D/polyvinylidenedifluoride composites. *Appl. Phys. Lett.* **2002**, *81*, 100–101. [CrossRef]

173. Lu, S.; Jin, J.; Zhou, X.; Fang, Z.; Wang, Q.; Zhang, Q. Large magnetoelectric coupling coefficient in poly(vinylidene fluoride-hexafluoropropylene)/Metglas laminates. *J. Appl. Phys.* **2011**, *110*, 104103. [CrossRef]

174. Lee, M.; Chen, C.Y.; Wang, S.; Cha, S.N.; Park, Y.J.; Kim, J.M.; Chou, L.J.; Wang, Z.L. A hybrid piezoelectric structure for wearable nanogenerators. *Adv. Mater.* **2012**, *24*, 1759–1764. [CrossRef] [PubMed]

175. Kim, H.S.; Kim, J.-H.; Kim, J. A review of piezoelectric energy harvesting based on vibration. *Int. J. Precis. Eng. Manuf.* **2011**, *12*, 1129–1141. [CrossRef]

176. Vatansever, D.; Hadimani, R.; Shah, T.; Siores, E. An investigation of energy harvesting from renewable sources with PVDF andPZT. *Smart Mater. Struct.* **2011**, *20*, 055019. [CrossRef]

177. Gusarov, B.; Gusarova, E.; Viala, B.; Gimeno, L.; Boisseau, S.; Cugat, O.; Vandelle, E.; Louison, B. Thermal energy harvesting by piezoelectric PVDF polymer coupled with shape memory alloy. *Sens. Actuators A Phys.* **2016**, *243*, 175–181. [CrossRef]

178. Tamang, A.; Ghosh, S.K.; Garain, S.; Alam, M.M.; Haeberle, J.; Henkel, K.; Schmeisser, D.; Mandal, D. DNA-Assisted β phase nucleation and alignment of molecular dipoles in PVDF film: A realization of self-poled bioinspired flexible polymer nanogenerator for portable electronic devices. *ACS Appl. Mater. Interfaces* **2015**, *7*, 16143–16147. [CrossRef] [PubMed]

179. Alluri, N.R.; Saravanakumar, B.; Kim, S.-J. Flexible, Hybrid Piezoelectric Film $(BaTi_{(1-x)}Zr_xO_3)$/PVDF Nanogenerator as a Self-Powered Fluid Velocity Sensor. *ACS Appl. Mater. Interfaces* **2015**, *7*, 9831–9840. [CrossRef] [PubMed]

180. Granstrom, J.; Feenstra, J.; Sodano, H.A.; Farinholt, K. Energy harvesting from a backpack instrumented with piezoelectric shoulder straps. *Smart Mater. Struct.* **2007**, *16*, 1810. [CrossRef]

181. Farinholt, K.M.; Pedrazas, N.A.; Schluneker, D.M.; Burt, D.W.; Farrar, C.R. An energy harvesting comparison of piezoelectric and ionically conductive polymers. *J. Intell. Mater. Syst. Struct.* **2009**, *20*, 633–642. [CrossRef]

182. Sun, C.; Shi, J.; Bayerl, D.J.; Wang, X. PVDF microbelts for harvesting energy from respiration. *Energy Environ. Sci.* **2011**, *4*, 4508–4512. [CrossRef]

183. Li, S.; Crovetto, A.; Peng, Z.; Zhang, A.; Hansen, O.; Wang, M.; Li, X.; Wang, F. Bi-resonant structure with piezoelectric PVDF films for energy harvesting from random vibration sources at low frequency. *Sens. Actuators A Phys.* **2016**, *247*, 547–554. [CrossRef]

184. Lovinger, A.J. Ferroelectric polymers. *Science* **1983**, *220*, 1115–1121. [CrossRef] [PubMed]

185. Pi, Z.; Zhang, J.; Wen, C.; Zhang, Z.-B.; Wu, D. Flexible piezoelectric nanogenerator made of poly(vinylidenefluoride-*co*-trifluoroethylene) (PVDF-TrFE) thin film. *Nano Energy* **2014**, *7*, 33–41. [CrossRef]

186. Lallart, M.; Cottinet, P.-J.; Lebrun, L.; Guiffard, B.; Guyomar, D. Evaluation of energy harvesting performance of electrostrictive polymer and carbon-filled terpolymer composites. *J. Appl. Phys.* **2010**, *108*, 034901. [CrossRef]

187. Cottinet, P.-J.; Lallart, M.; Guyomar, D.; Guiffard, B.; Lebrun, L.; Sebald, G.; Putson, C. Analysis of AC-DC conversion for energy harvesting using an electrostrictive polymer P(VDF-TrFE-CFE). *IEEE Trans. Ultrason. Ferroelectr. Freq. Control* **2011**, *58*. [CrossRef] [PubMed]

188. Shamos, M.H.; Lavine, L.S. Piezoelectricity as a fundamental property of biological tissues. *Nature* **1967**, *213*, 267. [CrossRef] [PubMed]

189. Telega, J.J.; Wojnar, R. Piezoelectric effects in biological tissues. *J. Theor. Appl. Mech.* **2002**, *40*, 723–759.

190. Chang, H.; Wang, Y. *Regenerative Medicine and Tissue Engineering—Cells and Biomaterials*; InTech: Rijeka, Croatia, 2011; pp. 569–588.

191. Marques, L.; Holgado, L.A.; Simões, R.D.; Pereira, J.D.; Floriano, J.F.; Mota, L.S.; Graeff, C.F.; Constantino, C.J.; Rodriguez-Perez, M.; Matsumoto, M. Subcutaneous tissue reaction and cytotoxicity of polyvinylidene fluoride and polyvinylidene fluoride-trifluoroethylene blends associated with natural polymers. *J. Biomed. Mater. Res. Part B Appl. Biomater.* **2013**, *101*, 1284–1293. [CrossRef] [PubMed]

192. Ribeiro, C.; Sencadas, V.; Correia, D.M.; Lanceros-Méndez, S. Piezoelectric polymers as biomaterials for tissue engineering applications. *Colloids Surf. B Biointerfaces* **2015**, *136*, 46–55. [CrossRef] [PubMed]

193. Ma, Z.; Kotaki, M.; Inai, R.; Ramakrishna, S. Potential of nanofiber matrix as tissue-engineering scaffolds. *Tissue Eng.* **2005**, *11*, 101–109. [CrossRef] [PubMed]

194. Young, T.-H.; Lu, J.-N.; Lin, D.-J.; Chang, C.-L.; Chang, H.-H.; Cheng, L.-P. Immobilization of L-lysine on dense and porous poly(vinylidene fluoride) surfaces for neuron culture. *Desalination* **2008**, *234*, 134–143. [CrossRef]

195. Wang, J.K.; Xiong, G.M.; Luo, B.; Choo, C.C.; Yuan, S.; Tan, N.S.; Choong, C. Surface modification of PVDF using non-mammalian sources of collagen for enhancement of endothelial cell functionality. *J. Mater. Sci. Mater. Med.* **2016**, *27*, 45. [CrossRef] [PubMed]

196. Wang, F.; Tanaka, M.; Chonan, S. A PVDF piezopolymer sensor for unconstrained cardiorespiratory monitoring during sleep. *Int. J. Appl. Electromagn. Mech.* **2002**, *16*, 181–188.

197. Bohlén, M.; Bolton, K. Conformational studies of poly(vinylidene fluoride), poly(trifluoroethylene) and poly(vinylidene fluoride-*co*-trifluoroethylene) using density functional theory. *Phys. Chem. Chem. Phys.* **2014**, *16*, 12929–12939. [CrossRef] [PubMed]

198. Ortiz, E.; Cuan, A.; Badillo, C.; Cortés-Romero, C.; Wang, Q.; Norena, L. DFT study of ferroelectric properties of the copolymers: Poly(vinyleneflouride-trifluoroethylene) and poly(vinylidene fluoride-chlorotrifluoroethylene). *Int. J. Quantum Chem.* **2010**, *110*, 2411–2417. [CrossRef]

199. Wang, Z.-Y.; Fan, H.-Q.; Su, K.-H.; Wen, Z.-Y. Structure and piezoelectric properties of poly(vinylidene fluoride) studied by density functional theory. *Polymer* **2006**, *47*, 7988–7996. [CrossRef]

200. Holman, R.W.; Kavarnos, G.J. A molecular dynamics investigation of the structural characteristics of amorphous and annealed poly(vinylidene fluoride) and vinylidene fluoride-trifluoroethylene copolymers. *Polymer* **1996**, *37*, 1697–1701. [CrossRef]

201. Bohlén, M.; Bolton, K. Molecular dynamics studies of the influence of single wall carbon nanotubes on the mechanical properties of Poly(vinylidene fluoride). *Comput. Mater. Sci.* **2013**, *68*, 73–80. [CrossRef]

202. Satyanarayana, K.C.; Bohlén, M.; Lund, A.; Rychwalski, R.W.; Bolton, K. Analysis of the torsion angle distribution of poly(vinylidene fluoride) in the melt. *Polymer* **2012**, *53*, 1109–1114. [CrossRef]

203. López-Encarnación, J.M.; Burton, J.; Tsymbal, E.Y.; Velev, J.P. Organic multiferroic tunnel junctions with ferroelectric poly(vinylidene fluoride) barriers. *Nano Lett.* **2010**, *11*, 599–603. [CrossRef] [PubMed]

204. Velev, J.P.; López-Encarnación, J.M.; Burton, J.D.; Tsymbal, E.Y. Multiferroic tunnel junctions with poly(vinylidene fluoride). *Phys. Rev. B* **2012**, *85*, 125103. [CrossRef]

205. Liu, Y.; Genzer, J.; Dickey, M.D. "2D or not 2D": Shape-programming polymer sheets. *Prog. Polym. Sci.* **2016**, *52*, 79–106. [CrossRef]

206. Ionov, L. Biomimetic Hydrogel-Based Actuating Systems. *Adv. Funct. Mater.* **2013**, *23*, 4555–4570. [CrossRef]

207. Zhao, Q.; Dunlop, J.W.; Qiu, X.; Huang, F.; Zhang, Z.; Heyda, J.; Dzubiella, J.; Antonietti, M.; Yuan, J. An instant multi-responsive porous polymer actuator driven by solvent molecule sorption. *Nat. Commun.* **2014**, *5*, 4293. [CrossRef] [PubMed]

208. Arazoe, H.; Miyajima, D.; Akaike, K.; Araoka, F.; Sato, E.; Hikima, T.; Kawamoto, M.; Aida, T. An autonomous actuator driven by fluctuations in ambient humidity. *Nat. Mater.* **2016**, *15*, 1084–1089. [CrossRef] [PubMed]

209. Deng, H.; Dong, Y.; Zhang, C.; Xie, Y.; Zhang, C.; Lin, J. An instant responsive polymer driven by anisotropy of crystal phases. *Mater. Horiz.* **2018**, *5*, 99–107. [CrossRef]